Masters in Chemical Engineering

Separation of gaseous mixtures (Nitrogen-Methane-carbon dioxide) by adsorption using titanosilicate ETS-4

Master's Thesis

Developed in the course of

Development Project in Foreign Institution

Erica Doutel Costa

Chemical Engineering Department

Evaluator at FEUP: **Alírio Rodrigues**

Supervisors at UCM: **José António Delgado and Ismael Águeda**

July 2010

Acknowledgments

In the development of this Project there were several people that contributed one way or another to its success.

First of all, I would like to say that was a pleasure to be part of the Erasmus Program in Spain, especially here in Madrid, in the Complutense University. I would like to thank Prof. Ismael Águeda in a special way, for all the value that recognized in me. I also would like to thank to my supervisor Prof. José António Delgado for his help, advices and patience during the past five months.

I would like to thank to my office colleagues Alicia, Edu, Goretti, Ana, Maria, Ismael Dias, Manolo, Sultan, Pilar, Sophie, Kike, Cesar, Sergio and Santiago for the good disposition and ambient. I really enjoyed all the subjects that we have talked about.

I really would like to thank, in a particularly way, to all the Professors in DEQ for making me the engineer that I am now.

Thanks to all my Erasmus friends, here in Madrid, that supported me during these five months, especially to Vasiliky, Argyro, Estela, Elena, Ana Carolina, João, Filipe, Pedro, Gianpaolo, Giulio and Emanuelle. It was great all the days that we have been together making these five months ones of the best of my life.

Thanks to all my friends in Portugal for all support and help that they gave to me in this time and for all the five years we spent together, especially to Andre Maia, Sara, João Mendes, Marta Pimenta, Bruno Santos, Paula Dias, Sofia Rocha, António Leal, Isabel Gomes and Ricardo Teixeira.

Many thanks to my friend and roommate during Erasmus, Ana Catarina Duarte, for all the days we spent in Madrid, for all the help and the constant support. I really enjoyed all the moments that we've been trough in Spain, all the places that we went, our adventures and especially our life together.

In particular I would like to thank to my boyfriend, José Maçaira, for the constant patience, and all the encouragement that he gave me to accomplish this project. I enjoyed all the visits received and how together we have overcome this distance. Without you it would not be the same.

Finally to my dear parents, Helena and Luís, for the constant support you gave during all my life. Thanks for the education that you gave to me, the patience, and all the important values that you have passed to me. Without you I would not be the woman that I am today.

Resumo

A separação de azoto e metano é cada vez mais importante na indústria do gás natural. Existe uma grande quantidade de reservas de gás natural que não podem ser utilizadas na actualidade, devido ao seu elevado teor em azoto. O interesse da separação azoto/metano tem suscitado a procura de novos adsorventes, entre os quais os mais promissores são as Cliptinolites e a ETS-4.

A ETS-4 é um titanosilicato microporoso desenvolvido pela empresa *BASF*, cujo tamanho do poro pode ser modificado mediante aquecimento para melhorar a sua selectividade cinética na separação azoto/metano. A maioria dos estudos sobre ETS-4 utiliza cristais sintetizados por aquecimento convencional. A informação disponível sobre as propriedades da ETS-4, especialmente as propriedades difusionais necessárias para a concepção de um leito de adsorção a escala industrial, é escassa.

Neste projecto, os cristais de Na-ETS-4 foram sintetizados por aquecimento com microondas e foram trocados por estrôncio para obter Sr-ETS-4, utilizando também esta nova fonte de aquecimento. Antes da sua utilização nas experiências de adsorção, ambos os materiais foram desidratados para reduzir o seu tamanho de poro e modificar a sua selectividade na separação metano/azoto e metano /dióxido de carbono. Os parâmetros de adsorção e difusão de azoto, metano e dióxido de carbono nestes materiais foram estimados mediante a modelização de pulsos destes os gases através de um leito fixo de cristais de ETS-4.

Analisando os resultados obtidos, observa-se que os adsorventes Na-ETS-4 e Sr-ETS-4, são ambos eficazes para a separação azoto/metano, já que a selectividade referente ao azoto é 1.03 para Na-ETS-4 e 8.04 para SR-ETS-4. A separação dióxido de carbono/metano requer um melhoramento no seu estudo mas os adsorventes são ambos eficazes para o seu estudo, visto que a selectividade para o CO_2 é 1.13 para Na-ETS-4 e 2.50. As diferenças entre as isotérmicas de CH_4 e N_2 são evidentes e os valores das capacidades de adsorção para o azoto são muito superiores às capacidades de adsorção para o metano. Este resultados obtidos, sugerem que a temperatura de desidratação empregue em ambos os adsorventes promove a contracção necessária do poro para a sua aplicação na separação azoto/metano.

Palavras-chave (Tema): ETS-4, Metano, Azoto, Adsorção, Difusão

Abstract

The separation of nitrogen from methane is becoming increasingly important in the natural gas industry. There exists a large amount of natural gas reserves that cannot be used at present, because of their high nitrogen content. The interest of the nitrogen/methane separation has prompted the search of new adsorbents, among which ion-exchanged clinoptilolites and ETS-4 are the most promising ones.

ETS-4 is a microporous titanium silicate developed by Engelhard Corporation, which possesses a small pore network, the size of which can be reduced by heat treatment to improve its kinetic selectivity in nitrogen/methane separation. Most of the reported studies about ETS-4 employ crystals synthesized with conventional heating. Furthermore, information available on the adsorption properties of ETS-4, especially the diffusion properties necessary to design a commercial adsorption process, is scarce.

In this work, Na-ETS-4 crystals have been synthesized by microwave heating and have been exchanged with Strontium to obtain Sr-ETS-4 using also microwave heating. Both materials have been dehydrated to reduce their pore size in order to enhance the selectivity in methane / nitrogen separation. The adsorption and diffusion parameters of nitrogen and methane on these materials have been estimated by modeling the desorption breakthrough curves of both gases using a fixed bed of ETS-4 crystals.

Analyzing the results, it is observed that the adsorbent Na-ETS-4 and Sr-ETS-4, are both effective for the nitrogen / methane separation, since the selectivity for nitrogen is 1.03 in Na-ETS-4 and 8.04 in Sr-ETS-4. The adsorbents are also effective for the separation of carbon dioxide / methane mixtures, whereas the selectivity for CO_2 is 1.13 in Na-ETS-4 and 2.50 in Sr-ETS-4. The differences between the CH_4 and N_2 isotherms are evident and the values of adsorption capacities for nitrogen are much higher than the adsorption capacity for methane. The results suggest that the temperature of dehydration used in both adsorbents promotes contraction of the pore required for its application in separating nitrogen / methane.

Keywords: ETS-4, Methane, Nitrogen, Adsorption, Diffusion

List of Figures

List of tables

Table of contents

Notation and Glossary

C	Concentration in the gas phase	$Mol \cdot m^{-3}$
D_C	Diffusivity coefficient	$m^2 \cdot s^{-1}$
d_i	Diameter of bed	m
D_L	Axial dispersion coefficient	$m^2 \cdot s^{-1}$
E_{Diff}	Activation energy of diffusion	$kJ \cdot mol^{-1}$
K_H	Henry constant	$mol \cdot kg^{-1} \cdot Pa^{-1}$
K_0	Pre-exponential factor	Pa^{-1}
L	Length of bed	m
P	Pressure	Pa
Q	Volumetric flow	$m^3 \cdot s^{-1}$
q	Adsorbed concentration	$mol \cdot kg^{-1}$
q*	Adsorbed concentration in equilibrium with the gas phase	$mol \cdot kg^{-1}$
$\bar{q}$	Average concentration adsorbed	$mol \cdot kg^{-1}$
q_s	Maximum adsorbed concentration	$mol \cdot kg^{-1}$
R	Ideal gas constant	$8.31 J \cdot mol^{-1} \cdot K^{-1}$
r_c	Diffusional distance	m
r_p	Particle radius	m
T	Temperature	K
t	Time	s
u	Superficial velocity	$m \cdot s^{-1}$
V_T	Total volume	cm^3
x	Dimensionless axial coordinate	
x_r	Dimensionless radial coordinate	
ΔH	Adsorption enthalpy	$kJ \cdot mol^{-1}$

Letras gregas

θ	Angle of diffraction	
ε	Porosity of bed	
μ	Viscosity	Pa·s
ρ	Density	$Kg \cdot m^{-3}$

Índices

0	Initial
g	Gas
p	Particle

Lista de Siglas

LDF	Linear Driving Force
PSA	Pressure Swing Adsorption
DRX	X-ray diffraction
SEM-FEG	Scanning Electron Microscopy field emission

1 Introduction

1.1 Relevance and Motivation

With the way of life in modern society, the greatest source of energy used is based on hydrocarbons. This has caused on the planet the known greenhouse effect, due to the large amounts of carbon dioxide produced by burning petroleum fuels. However cost-effective ways of producing energy without contaminating the environment have been developed and it is reasonable to propose the use of methane, the lightest hydrocarbon and the one that produces less carbon dioxide per unit of energy generated.

For this, the natural gas has to be transported from deposits to the place of consumption (power plants, petrochemical plants, supply of cars, etc.). Currently this is done using pipelines or transport in methane carriers. In certain fields, the content of carbon dioxide and inert, which is most nitrogen, is much larger than the maximum quantities allowed and natural gas must be purified in order to enter the pipeline.

Currently there are several techniques in the industry that can be applied in this purification. The removal of carbon dioxide by absorption with MEA (monoethanolamine) is the most widely used method. In the case of the removal of nitrogen, separation is more complicated. The most used technique is the cryogenic separation: condenses methane and nitrogen is vented to the atmosphere. This process is about 10 times more expensive than the removal of carbon dioxide [1] and is generally supported by obtaining helium as a byproduct.

Currently for situations where contamination with nitrogen and carbon dioxide is large, it is desirable to have a compact technology for these situations. This work proposes the study of an alternative technology for separating N_2/CH_4 and CO_2/CH_4, with molecular sieves by cycles using PSA (Pressure Swing Adorption)[2]. Adsorption is an operation for separating the components of a fluid mixture by retaining one of them in a porous solid (adsorbent) that is visually controlled by transport of matter from the fluid phase to the solid. In the separation by adsorption molecular sieves are commonly used, which retain the interior components of similar molecular size to pore size of the sieve, while larger components are excluded.[3]

The adsorbent used in the present separation process for the mixtures Nitrogen / Methane and Carbon Dioxide / Methane by PSA was developed by Engelhard Corporation, who hold the patent.[4] This adsorbent is known as ETS-4 (Engelhard Titanosilicate, and now it belong to the company BASF) and it's adequate for the separation of these molecules (N_2,

CO_2, CH_4) and others of similar size, since you can adjust the pore size of adsorbent by dehydration. [5]

In this project there were conducted, in a fixed bed adsorption column, several experiments with nitrogen, methane and carbon dioxide in Na-ETS-4 and Sr-ETS-4, varying the temperature and flow rate. The crystals of Na-ETS-4 were synthesized using microwave heating and were then exchanged by Strontium to obtain Sr-ETS-4, also by heating with microwaves. Both materials were dried to reduce the size of the pore. The parameters of adsorption and diffusion of nitrogen, carbon dioxide and methane in these materials were estimated by modeling the pulse curves of both gases through a fixed bed of crystals of ETS-4.

1.2 Natural Gas

Natural Gas comes from the decomposition of sedimentary plant and animal origin, accumulated over many thousands of years. Natural gas is a nonrenewable energy source, comprising a mixture of light hydrocarbons as its main constituents, where methane has a stake of more than 70% by volume. The natural gas composition can vary greatly depending on factors relating to the field where the gas is produced, the production process, conditioning, processing and transport. The Natural gas is the cleaner fossil fuel-burning, since its combustion results in lower amounts of sulfur and nitrogen oxides (responsible for acid rain) and carbon dioxide (which is the one responsible for the greenhouse effect) than the rest of the fossil fuels[1]. Its characteristics as a "green" energy source also contribute greatly to increase this expectation, especially in large urban areas with air pollution problems.[6]

The natural gas is the third most used source of energy worldwide.

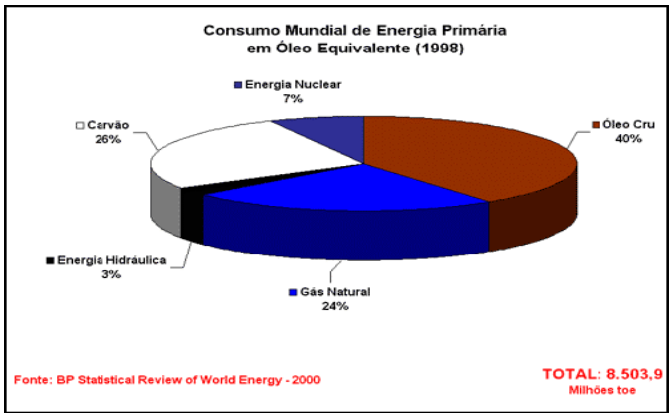

Figure 1: World consumption of natural gas compared to other sources primary energy [7]

At the present rate of consumption, natural gas reserves worldwide, only guarantee supplies for the next 60 years [8]. In the European Union this figure drops to 15 years, since it produces only 6.5% while consuming 16% of the total. It's a proven fact that major world

reserves are decreasing, making it necessary to seek new deposits of natural gas or even deposits of natural gas that is contaminated, due to its high content of nitrogen and carbon dioxide, that so far couldn't been explored. The nitrogen is a contaminant of natural gas, since it does not burn. A natural gas with high nitrogen content has a low calorific value, making it of poor quality in their usefulness as a fuel. The most popular technology for enrichment of natural gas is a cryogenic distillation [9], however, is only feasible when the flow of deposits to be extracted is very high. In deposits where you cannot achieve high rates of extraction, this technique is no longer profitable and the demand for new processes for the enrichment of natural gas is therefore a pending task.

Natural Gas utilization applications

The main applications of natural gas, after treated and processed, are in households, commerce, industries and vehicles. In countries with cold climate, the main use, whether is in private or commercial use, is in heating. In industry, natural gas is used as heat supply fuel, electricity generation and motive power, as a feedstock in chemical industries, petrochemicals ("steam reforming") and fertilizer (urea). In the area of transport, is used in buses and cars, replacing gasoline and diesel.

The use as fuel in vehicles, requires a high pressure compression (20 MPa), which makes the system expensive and dangerous. Another storage method that has received special attention, is adsorption, which turns out to be great promise for working with lower pressures (<4 MPa), providing the same capacity of compressed gas, since the density of adsorbed methane may be of the same order as the methane gas.[10] One problem affecting the efficiency of the adsorption process, that deserves mention, is the continued contamination of the adsorbent with the other constituents of natural gas, including CO2 and N2, which are considered as impurities in natural gas. Carbon dioxide is strongly adsorbed and can accumulate in the adsorbent bed, greatly reducing the adsorption of methane. Thus, more research is needed to the better performance in adsorption processes of natural gas, not only in the choice of adsorbents with higher adsorption capacity, but also with the study of the influence of other gaseous components in methane storage, with lowest possible costs.

1.3 Biogas

Biogas is a gaseous fuel with high energy content similar to natural gas, composed mainly of short chain linear hydrocarbons and consists on an average of 60% methane and 40% carbon dioxide, which is obtained by biological anaerobic degradation of organic waste. It can

be used for power generation, thermal or mechanical energy on a farm, helping to reduce production costs. The presence of water vapor, CO_2 and corrosive gases in biogas in nature constitutes the main problem in achieving its storage and production of energy. The removal of water, CO_2, hydrogen sulfide, sulfur and other elements through filters and devices for cooling, condensation and washing is essential for the reliability and use of biogas [11].

Biogas can be produced from nearly all kinds of organic materials. It is closely linked to agricultural activities and human consumption. Wherever there is a large population, and thereby a comprehensive quantity food production of a broad mixture of vegetable and animal foods, the right conditions exist for biogas production. In the future the large volume of biogas will be integrated into the European farming systems. There are quite a few biogas process volumes at the current wastewater treatment plants, landfill gas installations, and industrial biowaste processing facilities. However, the largest volume of produced biogas will, by 2020, be originated from farm biogas and from large co-digestion biogas plants, integrated into the arming- and food-processing structures.

Biogas utilization applications

Biogas can be utilized in several ways. It can either be applied raw or upgraded, but in minimum it has to be cooled, drained and dried right after production, and most likely it has to be cleaned for the content of H_2S as well, which in a short time interval will corrode the energy conversion technologies if the H_2S content is above 500 ppm.

There are various ways of biogas utilization:

- Production of heat and/or steam
- Electricity production / combined heat and power production (CHP)
- Industrial energy source for heat, steam and/or electricity and cooling
- Vehicle fuel
- Production of Chemicals
- Fuel cells

It can be fuelled to generate heat and/or electricity or applications of combined heat and power(CHP) plants and upgraded to vehicle fuel standards; these will be the most voluminous application routes. One case example of biogas for vehicle fuels is Sweden. The market for biogas as vehicle fuels has been growing rapidly the last 2-3 years. Today there are 12.000

vehicles driving on upgraded biogas/natural gas and the forecasts predicts 500 filling stations and 70.000 vehicles by 2010 [12].

2 State of the Art

2.1 Importance of Natural Gas

Global demand for energy has increased over the past 150 years, accompanying industrial development and population growth. Experts predict that the thirst for energy will continue to grow at least 50% by 2030 as developing countries like China and India seek to maintain its rapid economic growth. The biggest sources of world energy (responsible for 80% of energy consumed in the world at the moment) are coal, oil and natural gas - the so-called "fossil fuels" because they appeared centuries ago from the remains of plants and animals dead which are rich in carbon. However, those are sources that will one day be exhausted. [13]

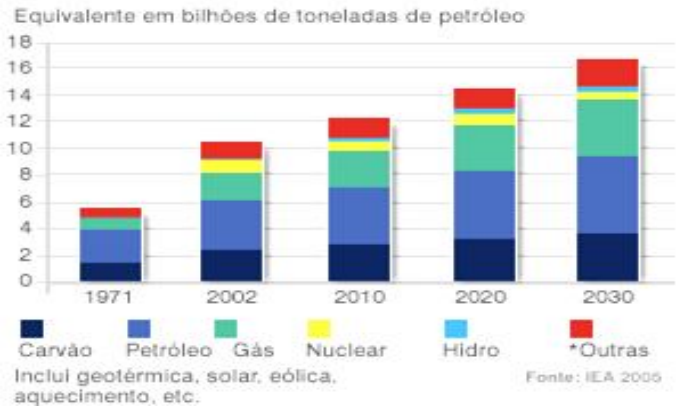

Figure 2: Estimated Future Energy demand. [13]

Natural gas is ranked third in the world's primary energy sources used and represents more than one fifth of the energy consumption both in Europe and worldwide.

The main factors that drive natural gas consumption in the world are:

- Increasing reserves, amounting to roughly 60% of oil reserves;
- More than 50 producing countries, creating an important flow of international trade;
- The possibility of reducing oil dependency.

Many signs indicate that the gas reserves in the world are far greater in number than those of oil and coal, since it can be found in nature with these two elements or derived from them, depending on their origin. The discovery of natural gas reserves increases continuously. Regularly are found out new deposits, and new extraction techniques that allow the drilling at even deeper depths. This increase in reserves converts natural gas into the

most used energy at the moment and which will have the greatest demand in the XXI century.

At the present rate of consumption, natural gas reserves in the world only guarantee supplies for the next 60 years. This figure drops up to 15 years for the European Union.

Natural gas is the second most important energy source in the European Union after oil, covering one quarter of total energy needs. It is estimated that natural gas consumption increases 26% by 2020, suffering simultaneously a decrease of 43% in production. In this sense, it is expected that Europe has to invest 25 billion Euros in infrastructures to ensure the supply of gas in the long term. [14]

2.2 The importance of the Separation Process

The separation of nitrogen and methane is becoming increasingly more important in the natural gas industry for the purification of natural gas for enhanced oil recovery. To be transported by a pipeline, natural gas must be treated and thus meet the specifications of transport. One of the most popular standards is one of the United States, the U.S. pipeline natural gas grid, where it's stated that the natural gas should have less than 4% of inerts and 2% of carbon dioxide in order to be fed into a pipeline. If the values of these components are higher than the ones stated, the first step is to remove the carbon dioxide by absorption with MEA, so the cryogenic separation of methane and nitrogen can be done in the nitrogen rejection unit, NRU.

For removal of nitrogen new technologies only began to appear in recent years. The cryogenic separation is very effective, but the energy costs are high and for the purified methane to be inserted into the pipeline it has to be recompressed, which involves in the same process two major stages of compression. There are at least three new alternatives to this. A PSA process commercialized in 2002 by the company Engelhard[15], using as adsorbent titanosilicates with barium and strontium that act as molecular sieves and in which relies this study.

For removal of CO_2 is also possible through the separation membranes [16]. A technology that appeared in the year 2001 is the PSA process of that uses as adsorbent titanosilicates [15]. The methane and inert gases are not selectively adsorbed and the process can reach the limit of <2% CO_2 required.

In the case of natural gas recompressing large part of the supply current in the adsorbed solvent is required, so that the method is only profitable if there are available large amounts of nitrogen. [1]

It's a proven fact that major world reserves are decreasing, making it necessary to seek new deposits or deposits of natural gas contaminated. In this sense, the study of separation by adsorption N_2/CH_4, is of vital importance for its use as an energy source.

2.3 Natural Gas in Portugal

The natural gas sector in Portugal is characterized by the absence of national production, from which rises the need for imports. The activity of importing natural gas is the conclusion of contracts with producers and operators of natural gas. [17]

Currently there are two contracts of long-term supply of natural gas, *Sonatrach*, the Algerian company, and with the NLNG, a Nigerian company. The first for the supply of gas through the pipeline from North Africa and the second in the form of liquefied gas by methane carriers.

In Portugal, natural gas was introduced in 1997 and in 1998 and has already a stake of about 4% of primary energy consumption.

It is estimated that natural gas consumption in Portugal will have an increase of 8% by 2010 and 7% by 2015, well above the European average. According to several authors, the natural gas market in Portugal is expected to grow from 4.4 billion cubic meters (m3) in 2006 to 8.5 billion m3 in 2015. [18]

For Portugal, a country that imports natural gas, the separation process by adsorption of nitrogen / methane also assumes an important role since it allows reducing the import of gas and therefore continuing their growth internally.

2.4 Separation methods

There are different techniques for separating N_2/CH_4. Most of the existing procedures for the retention of nitrogen are based on cryogenic distillation processes, but because they are not economically viable, except when dealing high flows, new technologies are being sought to replace them.

The cryogenic distillation process consists on many steps and involves high energy expenditure. It requires pretreatment of the natural gas stream to remove vapor, carbon dioxide, hydrocarbons and heavy aromatics that may condense during the process and cause problems. [19]

An alternative technology for the separation of N_2/CH_4 is the separation by adsorption through the use of molecular sieves. This adsorption is based on separation by molecular exclusion, in which the components with a molecular size similar to the pore of the sieve are trapped inside, while the larger components are excluded.

The adsorption has become an important tool for separation of such gas mixtures, and the most technological development in this area has been in the PSA (Pressure Swing Adsorption) process. PSA is a cyclic process that uses an adsorbent to allow the selective adsorption of one or more gases. Normally this process is used for separating the less adsorbed components but there are cases where the more adsorbed component is the wanted product [20] (Da Silva, 1999). Excellent introductions of the process of PSA have been made by Ruthven (1984) [21], Wankat and Tondeur (1985) [22], Yang (1987) [23] and Suzuki (1990) [24] .

Some examples of the use of PSA in the industry are the drying of natural gas, purification of hydrogen, air separation for N_2 with CMS and zeolites for oxygen. Wankat and Nataraj (1982)[25] suggested a PSA cycle for the separation of a ternary mixture of nitrogen, ethylene and acetylene. Cen et. Al (1985) [26] conducted a theoretical and experimental separation of a mixture of H_2, CH_4 and H_2S. The most important factor to achieve adequate separation, is the correct choice of adsorbent and the selection of the optimal operating conditions.

2.5 Titanosilicates

For an adsorption process to be viable there is the need of an adsorbent with high capacity, selectivity and lifetime.[27] It also should offer little resistance to the transfer of matter and it should be easily regenerated. In industry large quantities of adsorbents are used, where the most common are activated carbons, alumina and zeolites.

The first bibliographic references of the synthesis of titanosilicates are related to the incorporation of titanium in the structure of zeolite ZSM-5, giving rise to TS-1 (Taramasso et al., 1983). Other authors (Reddy et al., 1992) synthesized the known as TS-2, which has a topology MEL (ZSM-11). That same year, Davis (Davis, 1992) incorporated titanium in the structure of ZSM-48 Zeolite and Kuznicki et al., who, backed by the company Engelhard Corporation, developed a new family of titanosilicates known as ETS (Engelhard titanosilicate), at which the material ETS-4 (Kuznicki, 1990 and Kuznicki et al., 2000) ETS-10 (Anderson et al., 1994) and ETS-6 (Kuznicki et al., 2003) are its main contributions.

The ETS titanosilicates are a family of microporous crystalline materials, whose applications are similar to the zeolites mentioned above, but their properties are different mainly due to:

- they are made of titanium and silicon oxides;
- the titanium atoms have an octahedral and tetrahedral cordination in the silicon atoms;

- They framework can be reversibly dehydrated, varying the size of the pores (when the temperature of dehydration does not exceed a threshold value), without destroying its structure.

2.5.1 ETS-4

In 1989 (Kuznicki) were published two separate articles dealing with the structure of a synthetic material that resembled the mineral zorite. The material synthesized by Kuznicki was called ETS-4 (Na-ETS-4)[28] , and was thermally unstable and presented very bad absorption properties. Later, this same author demonstrated that the exchange of sodium cations in ETS-4 by strontium, made the structure more stable [28]. This new composition of ETS-4 (Sr-ETS-4) could become dehydrated by varying the pore size. This possibility of variation in the size of the pore has opened the doors for the synthesis of new molecular sieves such as ETS and ETS-6-10.The material synthesized by Kuznicki, is protected by a patent owned by U.S.firm Engelhard Corporation, hence the name "Engelhard Titanosilicate",and now, this company belongs to BASF. Improvements to the patented material (US-6, 068,682) were also developed in the same company. [29]

The synthesis of the material has the aim of application for the separation of N_2 from natural gas, since this material (the family of titanosilicates) has excellent surface properties and has adjustable pore size.The size can be adjusted with an accuracy of 0.1 Å. Therefore, the possibility of synthesizing a material with a uniform pore size and defined so precisely is of great importance in adsorption processes by exclusion (molecular sieve effect).

The company Engelhard Corporation developed a process of separation of N_2 and CO_2 from natural gas to enrich it into methane. This process is known as *Molecular Gate ® Adsoprtion-based System* [19], where the ETS-4 is the base system. The N_2 and CH_4 have a very similar size, 3.6 Å and 3.8 Å, respectively. ETS-4, as its pore size can be set to 3.7 Å, allows the passage of N_2 in its structure but prevents the passage of CH_4, which continues the chain of natural gas.[30]

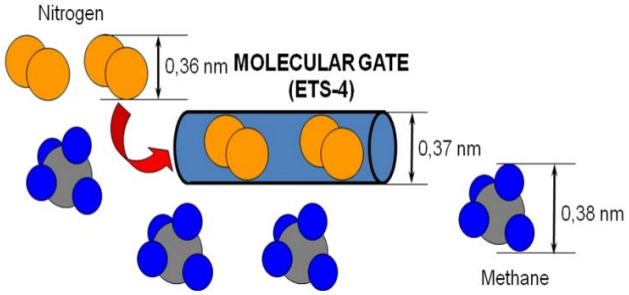

Figure 3: Scheme of operation of molecular sieve ETS-4.[19]

In the sieve the nitrogen molecules are not the only ones that are adsorbed, but also the molecules with inferior size to the pore of the adsorbent structure. CO_2 (3,3 Å) and H_2O (2,7 Å) are examples of such molecules. The material regeneration can be done by varying the pressure (*Pressure Swing Adsorption, PSA*).

2.6 Studies on adsorption and diffusion parameters

The information available on the adsorption properties of ETS-4, and particularly their diffusional properties is very scarce.

Jayaraman et al. (2004) [30] first published an article, where they obtained the isothermal and diffusional constant nitrogen and methane on Sr-ETS-4 synthesized using conventional heating.[6]

Marathe et al. (2005) [31] studied the adsorption equilibrium and kinetics of nitrogen and methane in Na-ETS-4 and Sr-ETS-4 in the form of pellets with a volumetric method, taking into account the effect of temperature, dehydration, and obtaining the corresponding parameters of the sorption and diffusion. Both the synthesis and ion exchange in this study was carried out using conventional heating.

Delgado et al. (2008) [32] also published an article, which studied the adsorption and the calculation of diffusional parameters of nitrogen and methane in ETS-4 synthesized by microwave heating and exchanged with strontium for Sr-ETS-4, also using heating microwave. The advantage of presenting a synthesis through the use of microwaves is to reduce the times of synthesis and ion exchange. It was found that the adsorption of methane was higher than that of nitrogen in Na-ETS-4, due to its large polarizability. The adsorbent exchanged with strontium, the nitrogen adsorption was stronger than that the one of methane, proving that the heat treatment at 200 ° C, promoted the contraction required for its application in separating nitrogen / methane. The ratio between diffusivities of nitrogen and methane obtained at 298 K are higher for Sr-ETS-4 due to shrinkage of the pore that prevents adsorption of methane.

Cavenati et al. (2009) [38] synthesized sodium titanosilicate (Na-ETS-4) and studied the effect of exchanging Na with different alkali-earth cations in the structure, namely Sr and Ca. These authors also studied the adsorption equilibrium of CH4 and N2 and CO2 and the effect of different activation temperatures. They found that the adsorption capacity of all gases is affected reflecting a contraction in the available volume for adsorption providing a strong evidence of the pore shrinking of the structure of the adsorbent.

3 Technical Description

3.1 General description of the installation

The experimental work regarding this was held in an experimental setup represented below. The installation consisted essentially of a gas supply system, an adsorption column, an analytical system of gas at the exit and a system for measuring flow discharge.

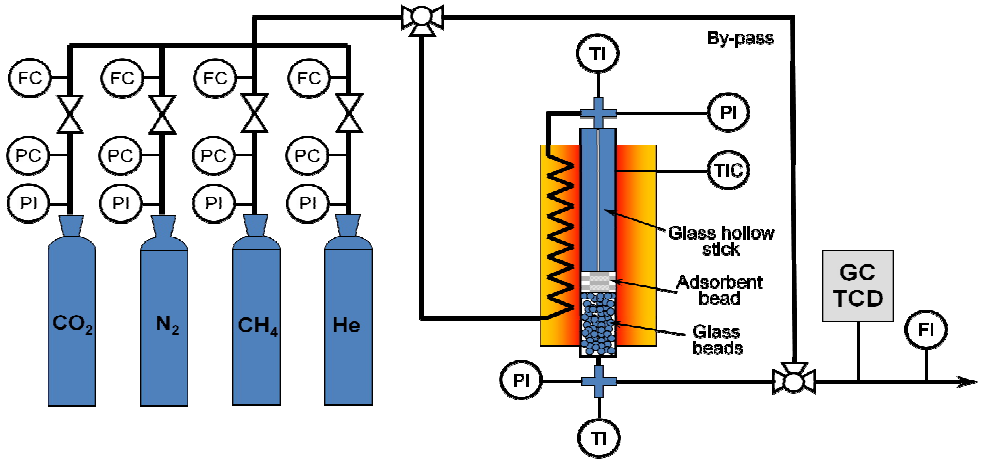

Figure 4: Diagram of the experimental setup procedure.

The gas supply system, comprises:

- Storage of gas cylinders used (supplier PRAXAIR) Helium (99.99%), nitrogen (99.99%), Methane (99.995%) and Carbon Dioxide (99.99%).
- Mass flow controllers for each of the input lines of gases, Bronkhost. Control box Model FC31 PKI process control.
- Two three-way electro valves: the first allows conducting the flow to the chromatograph and the adsorption bed and the second sends the gas flow from the line before or next the adsorption bed to the chromatograph. In the entire plant is used in stainless steel tubing 316.

Figure 6: Storage of gas cylinders

Figure 5: mass flow controllers

The adsorption column consists of the following parts:

▪ Fixed bed column of downward flow, where the bed with the adsorbent is placed. The column has an internal diameter of 0.9 cm and a length of 25 cm. The column is located inside an oven, where is placed a spiral pipe with an outside diameter with 2.24 cm, which is responsible for the thermal conditioning of the electric current fed to the bed.

▪ Heating system of the adsorption column, using a cylindrical steel electric oven and a refractory automatic temperature control. The maximum installed power is 1500W.

▪ Thermocouples Chromel-Alumel (Type K) to measure the temperature in the bed and in the oven. The thermocouples are connected to a Philips controller (Model KS40), which can be programmed manually or automatically to control action (ICT). The temperature controls acts on a circuit powered by an AC power supply (220V).

▪ Digital display where the temperature is shown in the bed and in the oven.

Figure 7: Images of the adsorption column.

The system of gas analysis outlet consists of:

- A gas chromatograph Varian CP-3800 equipped with a thermal conductivity detector (TCD).

- A software for registering the deterctor signal online and the integration of individual peaks.

Figure 8: Image of the gas chromatograph of the experimental setup.

Finally, the system for measuring gas flow outlet consists of a flowmeter.

3.2 Adsorption Isotherms

The adsorption experiments were carried out in the installation described above (Figure 4) and consist of the following steps:

Filling of the adsorbent bed and calcinations

First about 1 g of adsorbent is introduced into the column and in the top a 15 cm long glass rod is introduced to avoid dead volumes. Between both zones, a small amount of glass wool is placed to keep the independence between them. Then the adsorbent is calcinated in a helium atmosphere. The calcination temperature is 150 ° C (Na-ETS-4) and 200 ° C (Sr-ETS-4) during about 12 hours.

Preparation of feed mixture

When the calcination is finished, the installation is cooled to the temperature of adsorption. Once the temperature at which the process of adsorption-desorption will be carried out reached, and its value is stable, the mixture that will be fed into the adsorption stage is prepared. For that, it is introduced into the installation, without going through the bed, a flow of helium to be measured in the outlet. Then is mixed with a predetermined amount of adsorptive gas (methane, nitrogen or carbon dioxide) and the concentration of gas is analyzed in the chromatograph. The flow of adsorptive gas is determined by the difference between full flow and the flow of helium.

Adsorption

To carry out the adsorption is necessary to pass the feed along the bed. For this, there is a change in the three-way valves to the position at which the gas flows through the bed. When the concentration at the output of bed has the same value as the fed, the bed will be saturated. The gas flow is measured at the outlet.

Purge

After the adsorption experiment, the bed is deprived isolated through the exchange of the corresponding valves, allowing to pass the same flow of helium by the installation, by passing the bed. The stage ends when the concentration seen in the output indicates the presence of pure helium.

Desorption

The desorption of adsorbed gas is performed by passing helium through the bed. To achieve this, the operated three-way valves are put to the driving position to conduct just pure helium to bed. When the concentration measured is the same value as the one in the feed, the bed will be completely clean. The measured outlet flow of helium corresponds to the flow rate of desorption.

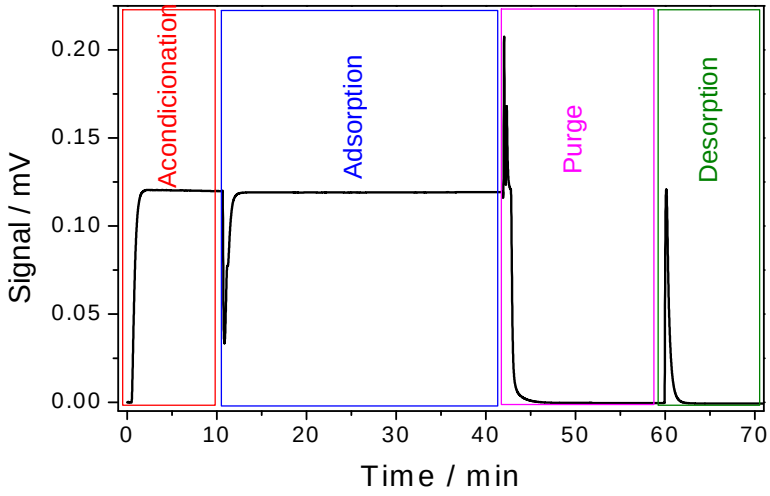

Figure 9: Stages of adsorption experiments.

3.3 Characterization techniques

The techniques used to characterize the synthesized materials are described below.

X-Ray Fluorescence (XRF)

The composition of the solids was determined by X-ray fluorescence (XRF). Analyses were performed at the Department of fluorescence at the Complutense University in Madrid, in an X-ray wavelength dispersive spectrometer Philips, Axios model with an x-ray tube, 4 kW Rh. The concentration of different elements was measured using their corresponding spectral lines in a vacuum using a 10 mm wafer diameter of corresponding samples.

Scanning Electron Microscopy field emission (FEG-SEM)

The morphology and crystal size of the prepared material were determined from photomicrographs taken in a scanning electron microscope of 30 kV field emission JEOL 6330 F, with a resolution of 12A and having a retrodispersed electron detector (BSE) and a microanalysis system (XEDS).

The samples were prepared by dispersing a small amount of material to be observed in acetone by ultrasound. Then they were deposited in a couple of drops of the mixture on a brass support and then the samples were left to dry for a few minutes. Due to the low electrical conductivity of the samples, they underwent a process of gold plating bath, using a Balzers SCD004 Sputter Coater for 5 minutes with an electric current of 20 mA at a pressure between 0:05-0:08 mbar.

3.4 Model Description

The model used to describe the dynamics of fixed bed adsorption is derived from mass balances, including the following assumptions:[33]

i. The flow pattern is described as an axial dispersion model followed by several tanks in series;

ii. The system is isothermal;

iii. The gas phase behaves as a mixture of ideal gases.

iv. The radial concentration and temperature gradients are negligible.

The balance of matter in the bed of adsorbent is represented by equation (1) with the following initial and boundary conditions:

$$\frac{\partial C}{\partial t} = \frac{D_L}{L^2}\frac{\partial^2 C}{\partial x^2} - \frac{u}{\epsilon L}\frac{\partial C}{\partial x} - \frac{1-\varepsilon}{\varepsilon}\cdot\rho_P\cdot\frac{\partial \bar{q}}{\partial t} \qquad \textbf{(1)}$$

$$\begin{cases} x = 0 & u(0 - C) = -\frac{D_L}{L}\varepsilon\frac{\partial C}{\partial x} \\ x = 1 & \frac{\partial C}{\partial x} = 0 \\ t = 0 & C = 0\ , \quad q = 0 \end{cases}$$

, where C is the adsorptive gas concentration in the gas phase (mol • m^{-3}), x is the dimensionless axial coordinate, D_L is the axial dispersion coefficient ($m^2 \cdot s^{-1}$), ρ_p the particle density (kg • m^{-3}), the bed porosity ε, $\bar{q}$ average adsorbed concentration.

The mass balance of the field in spherical particles is represented by equation 2 with the following boundary conditions:

$$\frac{\partial q}{\partial t} = \left(\frac{D_c}{r_c^2}\right)\cdot\left(\frac{1}{x_r^2}\cdot\frac{\partial}{\partial x_r}\left(x_r^2\frac{\partial q}{\partial x_r}\right)\right) \qquad \textbf{(2)}$$

$$\begin{cases} \dfrac{\partial \bar{q}}{\partial t} = \dfrac{3D_c}{r_c^2}\dfrac{\partial q}{\partial x_r}\Big|_{x_r=1} \\ x = 0 \quad , \quad \dfrac{\partial q}{\partial x_r} = 0 \\ x = 1 \quad , \quad q = q^* \end{cases}$$

, where x_r is the radial coordinate and dimensionless D_c diffusion coefficient ($m^2.s^{-1}$).

This model had to be improved since the original model did not describe the signal peak when using glass beads. In this sense there were observed a greater dispersion than that which the model predicts and so there were introduced to the output of the bed a number of stirred tanks to describe the signal obtained at the installation.

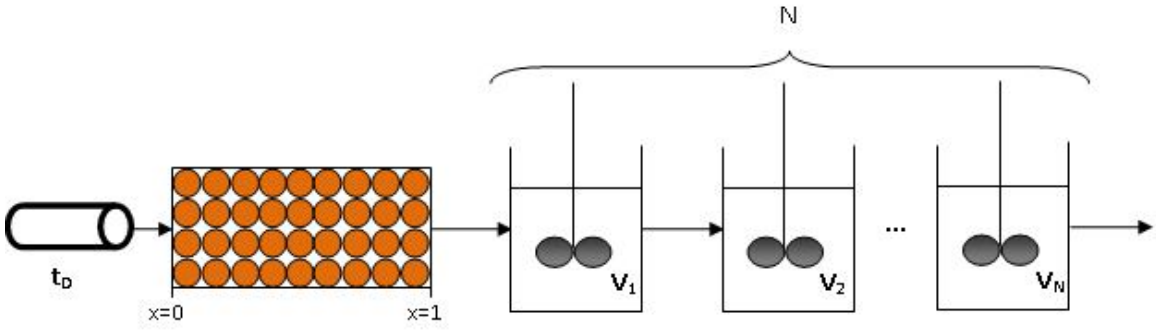

Figure 10: Schematic of the model used.

The mass balance in the tanks is described by the following equation:

$$\frac{dC_{Ti}}{dt} = (\mu \Pi r_x^2) \times \left(\frac{C_{Ti-1} - C_{Ti}}{V_T}\right) \qquad V_{T1} = V_{T2} = V_{TN} \qquad \textbf{(3)}$$

To solve this model we used a numerical method using the program PDECOL [35] (FORTRAN version 1978), a technique that uses orthogonal collocation in finite elements [36].

4 Results and discussion

4.1 Characteristics of the adsorbents used

In this project, there were used two different adsorbents, both of type ETS-4. These adsorbents were synthesized and characterized in the laboratories of the Chemical Engineering Department at the Complutense University in Madrid.

The synthesis was carried out taking into account the procedure described by Coutinho et al. [37], which uses silica gel as a silicium source and the following gel composition as starter:

$$8{,}5\ H_2O_2 : 2\ TiO_2 : 11{,}33\ SiO_2 : 16\ NaOH : 761\ H_2O$$

There were prepared two solutions, the first containing a quantity of soda dissolved in deionized water, where is added little by little, the silicium source, and the second solution is formed also by the rest of soda dissolved in to which is added drop by drop, the titanium source (titanium butoxide). To the second solution, is rapidly added hydrogen peroxide necessary to dissolve the white titanium precipitate formed.

Finally, the two solutions are mixed together with water needed to maintain the molar ratios, adding the dissolution that contains the source of titanium on the one that contains the silicon source. The set remains in agitation until the solution turbidity is eliminated.

The previously prepared gel is introduced in a teflon reactor of the microwave heating system, and remaining at a temperature of 200 ° C for 2 hours. Upon completion of the crystallization time, the solid formed is filtered and washed with deionized water until the pH of the water is neutral. Once washed it is dried at 70 ° C overnight.

The ion exchange is carried out using microwave heating. To do this, a 1 M solution of strontium chloride in deionized water is prepared, to which is added a quantity of material synthesized using a solid ration of 25 mL/ g. The temperature of the exchange is maintained at 200 º C for one hour.

Once finalized the exchange, the solid is filtered and washed with deionized water in abundance, until there is absence of Cl-ions in the water.

In the following table there are shown the values obtained from the analysis of X-ray fluorescence of the initial sample and the one exchanged with strontium, comparing the results with the results obtained in a previous study.

Table 1: Molecular formula of Na-ETS-4 and material exchange with Sr.

	Na-ETS-4		Sr-ETS-4		Na-ETS-4 (Delgado et al.)[32]	
	g/g·100	molar	g/g·100	molar	g/g·100	Molar
Ti	14,08	0,29	13,38	0,28	21.20	0.44
Si	21,06	0,75	19,14	0,68	22.80	0.81
O	50,98	3,19	45,73	2,86	44.98	2.81
Na	13,79	0,60	0,92	0,04	10.96	0.48
Cl	-	-	0,25	0,01	-	-
Sr	-	-	20,38	0,23	-	-
Others	0,1	-	0,2	-	0.053	-
Ti/Si		0,39		0,41		0.55
% Ion exchange		-		93		-

From the table, it can be observed that the ratio Ti / Si is lower than the previous study by Delgado et al [32]. The exchange procedure by microwave is very effective compared to conventional heating, as with a single exchange gives a degree of exchange of 93%, while other authors propose several exchanges for a similar degree of exchange as Marathe.[31]

First there was synthesized the adsorbent in the form of sodium (Na-ETS-4). This adsorbent has a large thermal instability because it looses its structure, above 150 ° C, as it is visible in the figure below, which analyzes the X-ray diffractogram at different temperatures.

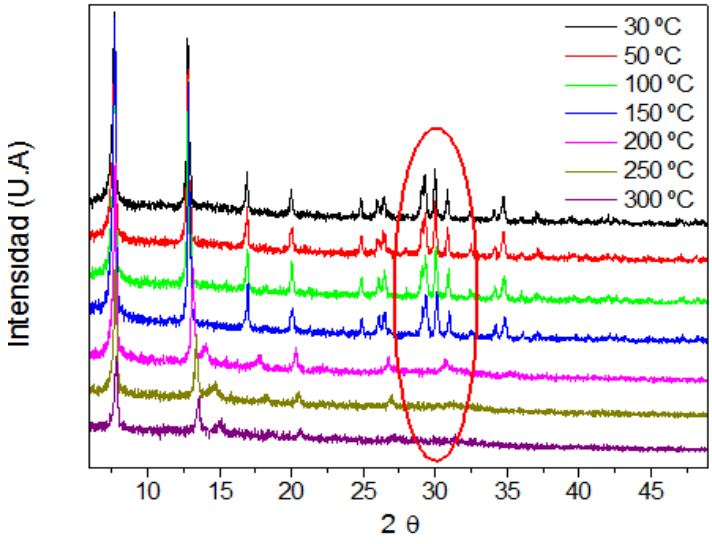

Figure 11: Influence of dehydration temperature on the structure of Na-ETS-4.

Dehydration at high temperatures has the objective of reducing the pore size of adsorbent so that you can use a molecular sieve in the separation of N_2, CH_4, CO_2.

The thermal instability presented by the sodium form adsorbent, makes necessary the exchange of sodium by strontium. In the next picture is analyzed the X-ray diffractogram in order to verify the influence of temperature of dehydration on the structure of the adsorbent Sr-ETS-4.

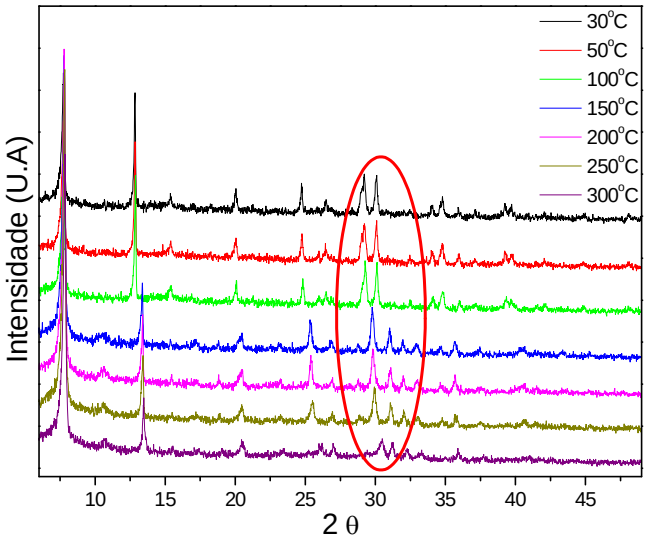

Figure 12: Influence of dehydration temperature on the structure of Sr-ETS-4.

Observing Figure 12, the structure that is exchanged with strontium has a higher thermal stability compared to their sodium form. The increase in temperature produces a drag of peaks for higher angles of diffraction, which implies a reduction of lattice dimensions, which is the same as the contraction of the pores of the material. Even so, there is a loss of crystallinity at temperatures higher than 250 ° C.

Additional studies show that up to 150 º C the sample dehydration is reversible. However, after treatment at 300 º C, the crystallinity of the starting material is not recovered.

The synthesized samples were analyzed using scanning electron microscopy (FEG SEM) and the micrographs obtained are shown in Figure 13. Note how the ETS-4 is constituted by blades that intersect to form particles with 10 mm radius. Each blade have rectangular dimensions of 10 mm in length, about 4-5 mm of width and a thickness less than 1 micrometers.

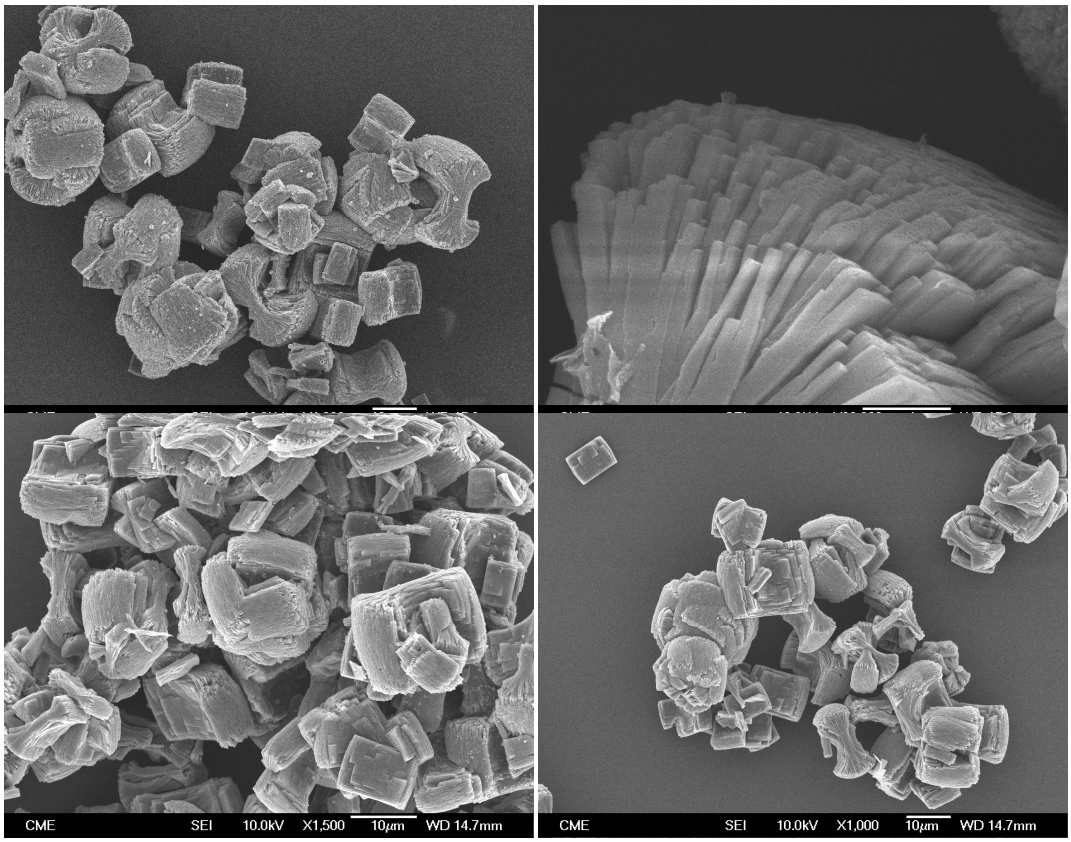

Figure 13: SEM images obtained from the synthesized adsorbents in this project.

4.2 Calibration

After all the equipment being properly mounted, it was introduced known concentracion pulses of methane, nitrogen and carbon dioxide, and then, it was observed the response of gases concentration in the TCD detector. It was realized experiments with 0.05, 0.1, 0.25, and 0.5 mL of N_2, CH_4 and CO_2, varying the helium flow at 30, 60 and 90 mL .min^{-1}, in order to verify the influence of helium flow in the TCD detector.

The figures below depict the calibration curves obtained for pulses of nitrogen, methane an carbon dioxide, respectively, modifying the helium flow.

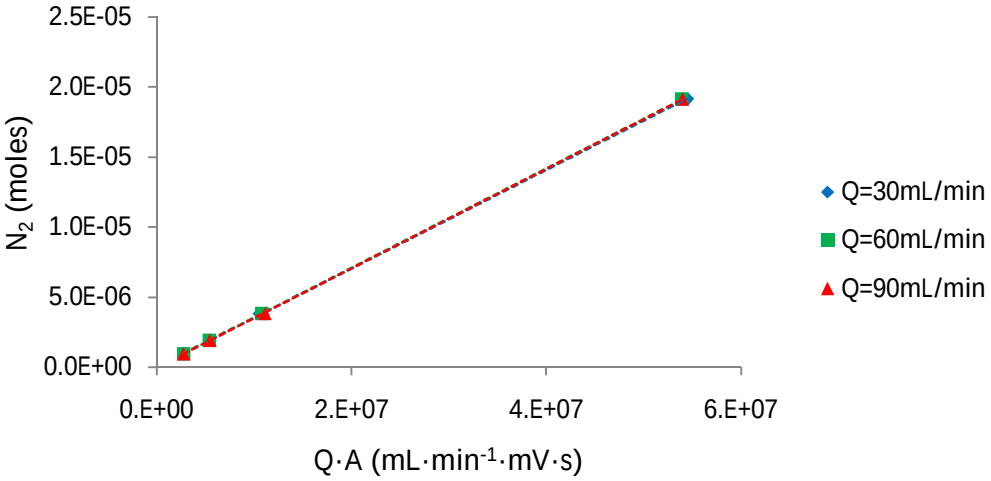

Figure 14: Calibration curve for pulse of N_2, varying the helium flow.

Where Q is the volumetric flow rate and A is the area below the peak.

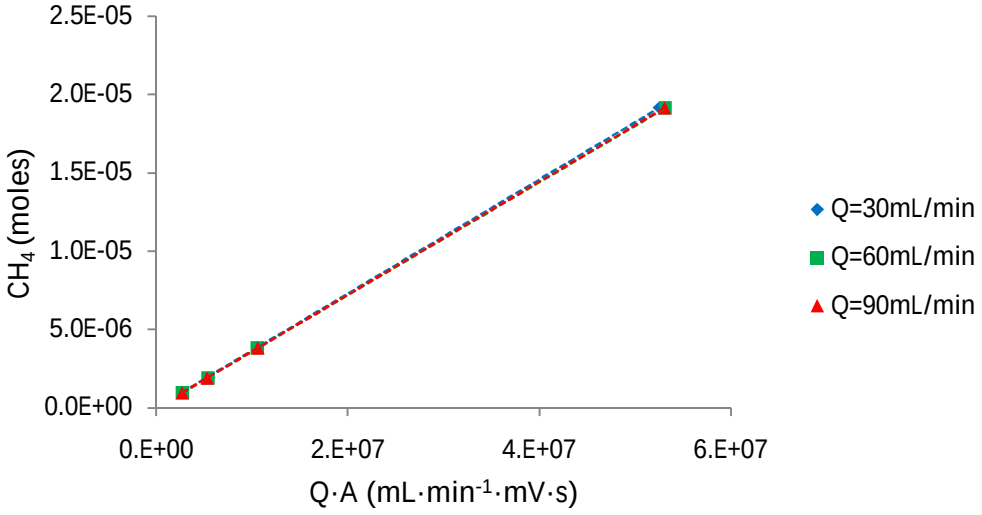

Figure 15: Calibration curve for pulse of CH_4, varying the helium flow.

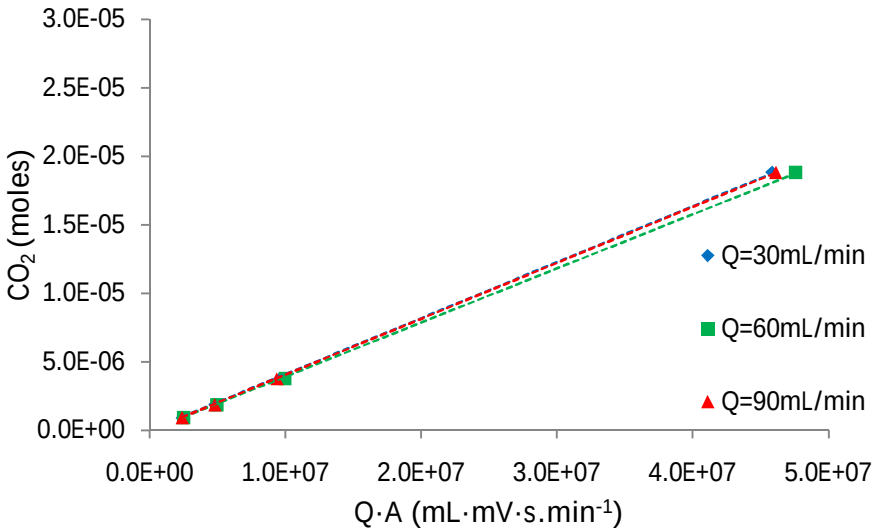

Figure 16: Calibration curve for pulse CO_2, varying the helium flow.

Through the analysis of the figures above, it can be concluded that for nitrogen, methane and carbon dioxide experiments the helium flow does not influence the TCD detector response.

4.3 Dead Volume

In order to estimate the adsorption and diffusion of the different gases in ETS-4, two different methods were used.

In the first method, the experimental desorption curves, allowing to estimate the equilibrium adsorption constants; and in the second one, it was used the model previously explained in chapter 3.4, allowing to estimate the equilibrium constant and the diffusion parameters, from the experimental pulse responses, simultaneously.

Either in one method or another, it was necessary to estimate properly the effect of dead volume in the experimental installation.

Thus, the dead volume obtained for the first model was given by Professor Ismael Águeda, and for that reason is out of this work ambit.

The experiments were performed with helium using a settled nitrogen flow (2.23 $mL.min^{-1}$) in the experiments of adsorption, assuming that helium is not adsorbed. Thus, several experiments were performed for several settled values of nitrogen flow, but varying the helium flow, where the dead volume obtained was $9.3.10^{-6}$ $mL.min^{-1}$. This value was used and kept constant in order to determine all the adsorption isotherms of this work.

For the second method, which it was calculated both the equilibrium constant of adsorption and diffusional parameters, it was also necessary to estimate the dead volume of the experimental installation. So, it was injected small amounts (0.1 mL) of helium to obtain pulses of helium, maintaining the nitrogen flow as constant, and also proposing a model of fixed bed with tanks in series (chapter 3.4) to simulate the signal of individual peaks obtained. Varying the number of tanks and each of its volume, in order to promote the best adjustment on the zone where diffusion has more influence. Thus, it was able to measure the time delay on the pipes verified before and after adsorption bed until reaching the TCD detector, this time translates into dead volume.

The parameters used to estimate the dead volume for the pulse method are given in table 2.

Table 2: Parameters to estimate the dead volume.

	Na-ETS-4	**Sr-ETS-4**
Length$_{Bed}$ (cm)	2.884	2.625
Mass of adsorbent(g)	1.137	1.013
Porosity $_{bed}$ (ε)	0.53	0.61
Density $_{bed}$(kg.m^{-3})	619.7	602.82
Density $_{particle}$ (kg.m^{-3})	1320	1530
Operation Temperature (K)	293	298
Operation Pressure (mm.Hg)	706	704.1

The figure below represents the obtained helium peaks for different settled helium flow at 298 K. The remaining simulations realized at other temperatures are given in Annex A.

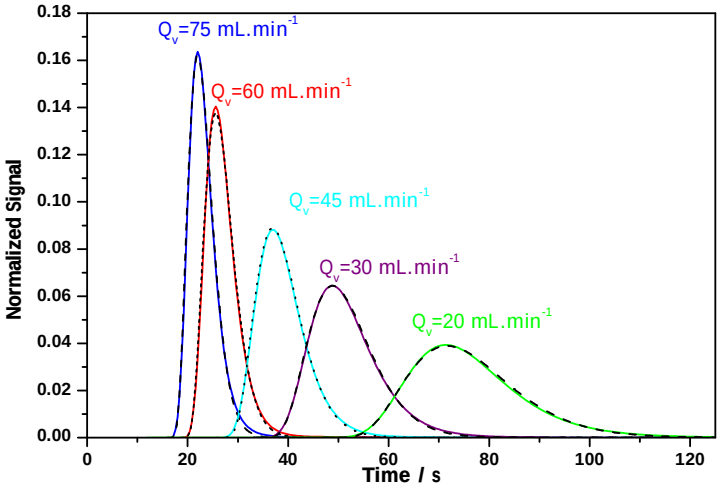

The solid lines correspond to experiments, and the dashed lines are the corresponding simulation

Figure 17: Adjustment of the helium peaks with QN_2=2.23mL.min^{-1} at 298 K.

According to this figure, it is observed that this model fits quite well the experimental pulses. These adjustments allowed to simulate the effect of dead volume present at the experimental installation, further necessary to calculate the adsorption and diffusion parameters. In the table below, it is summary described, the number of simulated tanks and their respective volumes, and then the determined dead volume through the obtained peaks of helium, varying the nitrogen flow, for all the experiments realized with helium.

Table 3: Simulations values to calculate the dead volume, in experiments with helium.

T (K)	Q_{N2} (mL.min^{-}1)	Nº Tanks	V_{Tanks} (mL)	Dead Volume before bed (mL)
298	76.9	7	1.38	20.30
	66.1		1.40	20.50
	54.7		1.42	19.50
	43.0		1.40	18.50
	32.4		1.45	18.20
308	21.7	7	1.35	21.40
	73.6		1.38	20.00
	63.3		1.45	19.50
	42.8		1.50	18.20
	32.2		1.60	17.00
	21.5		1.46	19.22
323	73.8	7	1.40	20.90
	62.8		1.40	20.20
	42.3		1.51	19.30
	31.8		1.57	18.60
	21.2		1.67	17.00

Analyzing such results it can be verified, as said above, that the model fits quite well the experimental results. It should be noticed that, as expected, the dead volume in the installation is independent of flow rate and temperature.

4.4 Adsorption Isotherms

The adsorption isotherm is an expression that relates the concentration of the adsorbed phase (qi) and the concentration of fluid phase, expressed in the form of partial pressure (Pi) in gaseous systems, at constant temperature for an adsorbate-adsorbent system.

The adsorption experiments for the calculation of adsorption isotherms were performed for the three gases, it should be emphasized that the carbon dioxide experiments were meaningless, since the results were inconclusive, so that will not appear in this part of this work. So, it was calculated the adsorption isotherms only for methane and nitrogen. It was determined the isotherms at different temperatures for the synthesized adsorbents in the range of compositions studied. These variables and the range of variation were as follows:

- **Adsorption temperature**:

Experiments were conducted at three different temperatures of adsorption: 298 K, 308 K and 323 K.

- **Composition of fed gas mixture:**

The molar fraction of N_2 and CH_4 in the feed ranged between 0-0.1 for Na-ETS-4 and Sr-ETS-4.

Below, it is depicted the equilibrium isotherms of nitrogen and methane in the adsorbent ETS-4, either in sodic form or in the exchanged with strontium form. It was obtained isotherms at three different temperatures, in order to calculate the adsorption enthalpy of the gases in each adsorbent.

4.4.1 Na-ETS-4

Firstly, it was conducted experiments with the adsorbent in the sodic form. The resulting isotherms are represented in the figures below:

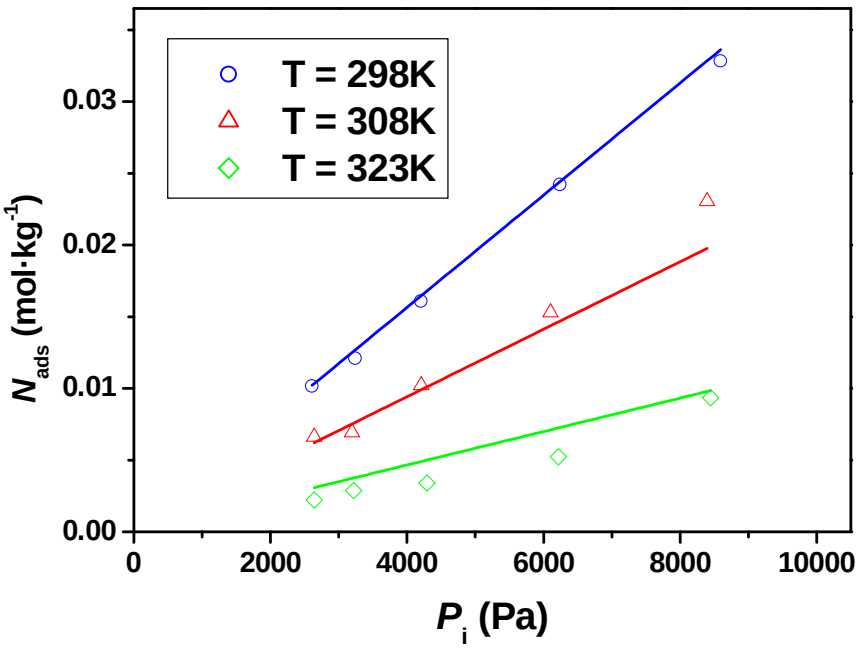

Figure 18: Adsorption isotherms for N_2 in Na-ETS-4.

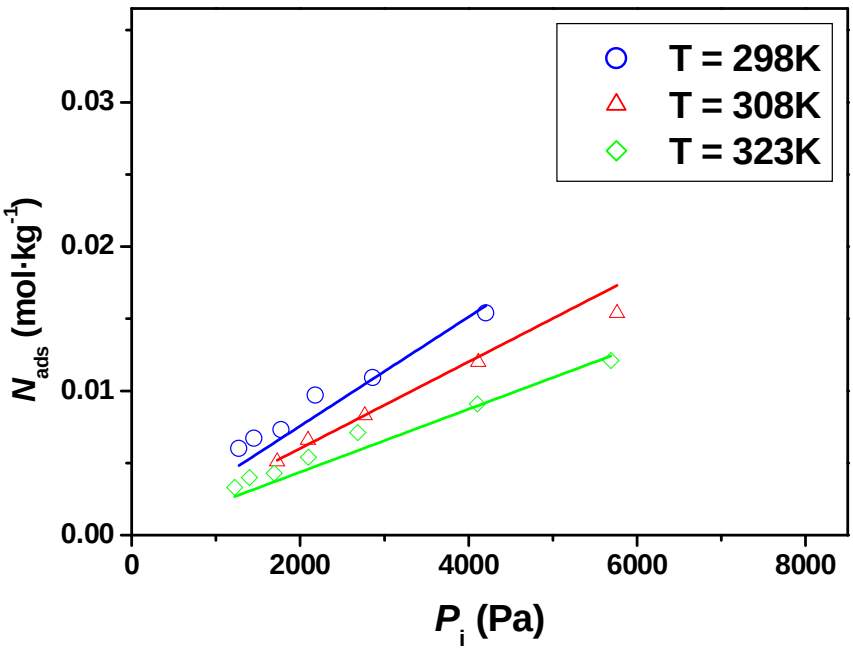

Figure 19: Adsorption isotherms for CH_4 in Na-ETS-4.

Analyzing the evolution of experimental points in the previous figures, it can be observe that in both, methane and nitrogen, the points fit to a linear isotherm of the Henry's type:

$$q_i = K_H . P_i \qquad K_H = K_0 . e^{(-\Delta H / RT)} \qquad \textbf{(4)}$$

where K_H is Henry's constant, which brings together the saturation capacity and equilibrium constant and is expressed in mol . kg $^{-1}$. Pa^{-1}, P_i is the partial pressure expressed in Pa, (-ΔH) is the adsorption enthalpy in kJ .mol^{-1} and K_0 is the pre-exponential factor in Pa^{-1}. Knowing the adsorption isotherms for both gases, it was necessary to realized a multiple linear adjustment, with the purpose of obtain the adsorption enthalpy (-ΔH) and the parameter K_0.

In the following table are the obtained parameters as the result of the multiple regressions carried out through the values of the isotherm of methane and nitrogen, with the adsorbent in the sodic form.

Table 4: Parameters obtained through the multiple regression performed for Na-ETS-4.

	Na-ETS-4		
	K_0	$-\Delta H$	r^2
	(Pa^{-1})	($kJ \cdot mol^{-1}$)	
CH_4	$3.13 \cdot 10^{-9}$	17.58	0,941
N_2	$6.27 \cdot 10^{-13}$	38.76	0,980

Obtaining the values K_0 and (-ΔH), and knowing that the isotherm is of Henry's type, then it was possible to calculate Henry's constant (K_H) and selectivity in the separation of the mixture N_2/CH_4 at different temperatures.

The selectivity or separation factor is very important for the choice of adsorbent to a separation process. The selectivity for a process controlled by the equilibrium is defined as (Ruthven et al., 1994), since $C_{Af}=C_{Bf}$:

$$\alpha_{AB} = \frac{q_A}{q_B} \quad \textbf{(5)}$$

where q_i is the adsorbed concentration of each component in mol . kg^{-1}. In the following table is depicted the values obtained for Henry's constant for both gases and their respective selectivity at different temperatures.

Table 5: Henry's constant in equilibrium and selectivity obtained for the adsorbent Na-ETS-4.

	Na-ETS4		
T	$K_{H,CH4}$	$K_{H,N2}$	$\alpha_{N2/CH4}$
(K)	($mol \cdot kg^{-1} \cdot Pa^{-1}$)	($mol \cdot kg^{-1} \cdot Pa^{-1}$)	
298.15	$3.77.10^{-6}$	$3.88.10^{-6}$	1.03
308.15	$2.99.10^{-6}$	$2.34.10^{-6}$	0.78
323.15	$2.18.10^{-6}$	$1.16.10^{-6}$	0.53

4.4.2 Sr-ETS-4

After all the experiences realized with the adsorbent Na-ETS-4, it was performed new ones with the adsorbent exchanged by strontium. The following figure represents the adsorption isotherms for both gases at different temperatures

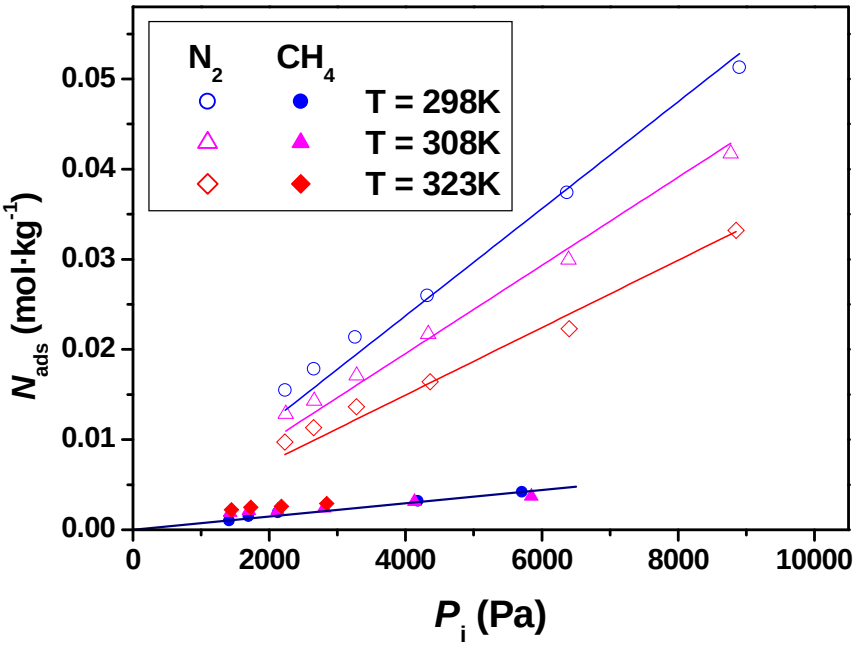

Figure 20: Adsorption isotherms for CH_4 e N_2 in Sr-ETS-4.

In the case of methane, it wasn't estimated the enthalpy parameters, neither K_0, because this gas is adsorbed in very small quantities so there was no clear dependence on the temperature.

As observed for the adsorbent in the sodic form, now both the nitrogen and methane, the experimental points can be fitted to a linear isotherm of the Henry's type. Table 6 depicts the parameters calculated, after being realized a multiple linear regression.

Table 6: Parameters obtained through the multiple regression carried out for Sr-ETS-4.

	Sr-ETS-4		
	K_0 (Pa^{-1})	$-\Delta H$ ($kJ \cdot mol^{-1}$)	r^2
CH_4	---	---	---
N_2	$1.50 \cdot 10^{-8}$	14.81	0.985

As expected, it can be verified that, with this adsorbent, unlike nitrogen, the methane is adsorbed in very small quantities.

Table 7: Equilibrium parameters and selectivity for the adsorbent Sr-ETS-4.

	Sr-ETS4		
T (K)	$K_{H,CH4}$ (mol·kg-1·Pa-1)	$K_{H,N2}$ (mol·kg-1·Pa-1)	$\alpha_{N2/CH4}$
298.15	$7.36.10^{-7}$	$5.92.10^{-6}$	8.04
308.15	$7.36.10^{-7}$	$4.87.10^{-6}$	6.62
323.15	$7.36.10^{-7}$	$3.73.10^{-6}$	5.06

The Henry's constant for methane was determined by making an adjust with zero and the last point, to enable a better fit for all points, since there was an high error with the influence of temperature.

4.5 Comparison Na-ETS-4 *versus* Sr-ETS-4

It was calculated the selectivity of the adsorbent in equilibrium, for the two gases under study at different temperatures. In the table below, is compared the obtained selectivity for each adsorbent:

Table 8: Selectivity in equilibrium for both adsorbents.

	Na-ETS4	Sr-ETS4
T (K)	$\alpha_{N2/CH4}$	$\alpha_{N2/CH4}$
298.15	1.03	8.04
308.15	0.78	6.62
323.15	0.53	5.06

Observing the results it can be verified that both gases are adsorbed in Na-ETS-4. On the other side, in Sr-ETS-4, the nitrogen is adsorbed in higher quantity than methane. The differences between the isotherms of CH_4 and N_2 are clear and the values of adsorption capacity for N_2 are much higher than the adsorption capacity for CH_4.

The adsorption enthalpy for nitrogen in Na-ETS-4 are superior than those obtained for the adsorbent Sr-ETS-4 due the repulsion creates by the pores in strontium, previously dehydrated, is higher so the enthalpy decreases. These values are quite different from those found in the literature, although the difference in the composition and different heat treatment may justify such differences found.

The increase of adsorption capacity of nitrogen in Sr-ETS-4 can be explained by the decreased occupancy of water with the heat treatment in this material and by the higher electric field induced by strontium.

4.6 Estimation of adsorption and diffusion parameters

In this work it was estimated simultaneously both the adsorption equilibrium constant, K_H, and the diffusional constant.

For the calculation of the constants is necessary to understand the diffusional coefficients of mass transfer (Dc), which were determined by adjusting the experiments of the three gases, passing a settle nitrogen flow, through the simulation of the mathematical model resorting to using the program PDECOL.

For the adjustment of the simulated curve is necessary to know the characteristics of the bed: length, density and porosity, as well as the mass and density of the particles of adsorbent. For each experiment in particular is also necessary to know the flow of desorption, molar fraction fed, operating temperature and operating pressure.

In the following table is shown in summary form, the characteristics of the bed and the characteristics of both adsorbents required for the simulation of experimental curves.

Table 9: Characteristics of adsorbents and bed.

	Na-ETS-4	**Sr-ETS-4**
Length$_{Bed}$ (cm)	2.884	2.625
Mass of adsorbent(g)	1.137	1.013
Porosity $_{bed}$ (ε)	0.53	0.61
Density $_{bed}$(kg.m^{-3})	619.7	602.82
Density $_{particle}$ (kg.m^{-3})	1320	1530
Operation Temperature (K)	295	299
Operation Pressure (mm.Hg)	704.1	702.7

Once known operating which the experimental curves were obtained, fits the curve simulated using the program PDECOL, having two parameters as variables, the diffusion parameters, (D_c/r_c^2) and the equilibrium adsorption constant K_H.

4.6.1 Na-ETS-4

In the figure below, are described examples of curve adjustments to the experimental nitrogen as adsorbent in sodium, for a given operating temperature. The other adjustments, the other temperatures are in the annexes.

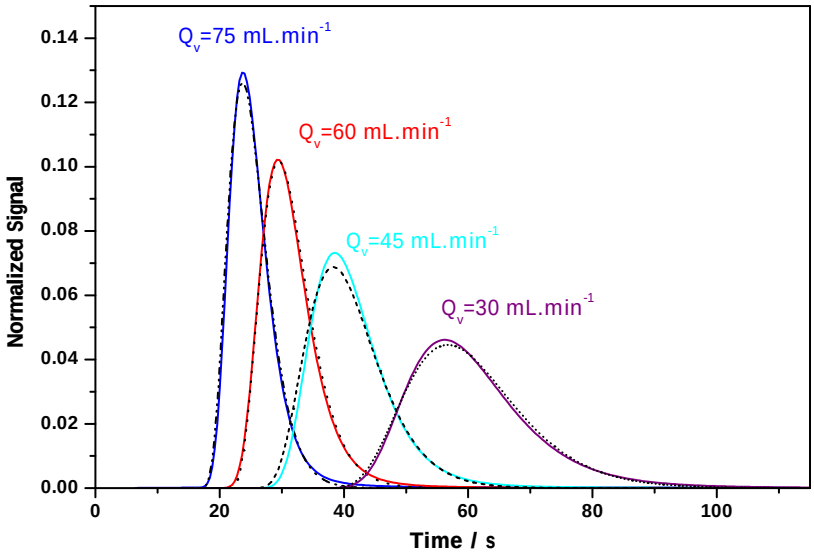

The solid lines correspond to experiments, and the dashed lines are the corresponding simulation

Figure 21: Adjustment of experimental curves of N_2 Na-ETS-4 at 25 ºC, varying helium flow.

Through figure 21, it can be observed, that the simulated curves fit well the experimental curves. Thus, it can be obtained reliable adsorption and diffusion parameters.

The following table depicts the values of adsorption and diffusion parameters for all experiments with nitrogen in Na-ETS-4.

Table 10: Diffusion and adsorption parameters obtained for experiments of N_2 in Na-ETS-4.

T (K)	Q_{He} (mL.min^{-1})	D_c/r_c^2 (s^{-1})	K_H (mol. (Kg.Pa)$^{-1}$)
298	77.1	0.068	$1.00.10^{-6}$
	61.9	0.053	$9.00.10^{-7}$
	46.6	0.050	$1.40.10^{-6}$
	31.7	0.043	$1.50.10^{-6}$
308	76.6	0.050	$4.00.10^{-7}$
	61.6	0.063	$7.20.10^{-7}$
	46.5	0.055	$7.00.10^{-7}$
	30.7	0.050	$7.50.10^{-7}$
323	76.4	0.075	$2.50.10^{-7}$
	60.6	0.075	$2.50.10^{-7}$
	45.5	0.088	$1.50.10^{-7}$

As expected for an adsorption process, the values of equilibrium constant, K_H, decrease as the temperature increases. On the other side, for mass transfer coefficient and diffusion it is verified that the increase on the temperature, make them increase too.

It was made a sensitivity study of the influence of diffusional parameters and the equilibrium adsorption constant, in the following figure it can be observed how these factors greatly influence the experimental adjust.

a) b)

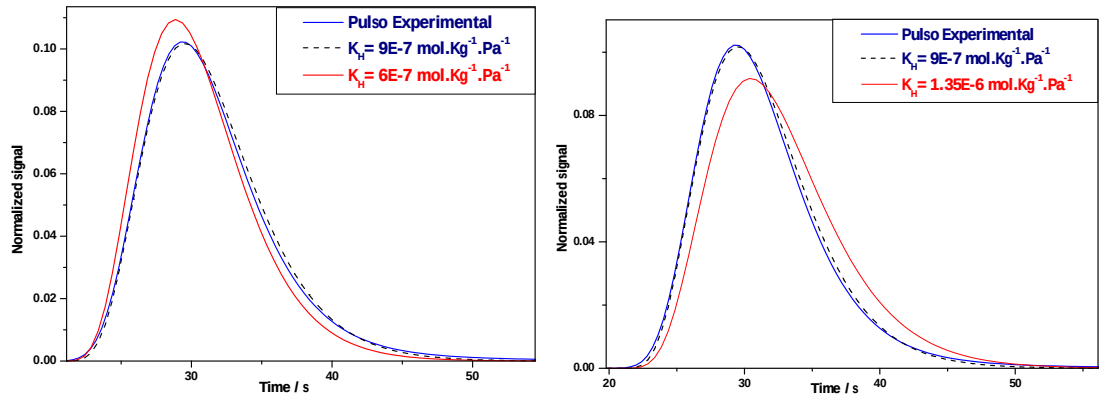

Figure 22: Representative adjustment of pulse of N_2 with a helium flow of 61.9mL.min^{-1} and D_c/r_c^2=0.053 s^{-1}, when **a)** decreasing the equilibrium constant of adsorption; **b)** increasing the equilibrium constant of adsorption.

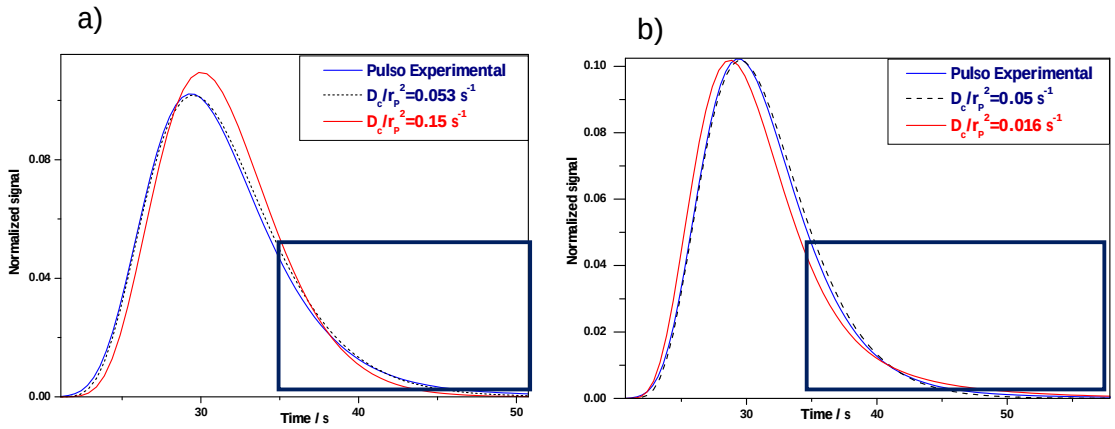

Figure 23: Representative adjustment of pulse of N_2 with a helium flow of 61.9mL.min^{-1} and K_H= 9.10^{-7} mol.Kg^{-1}.Pa^{-1}, **a)** increasing the diffusion parameters; **b**) reducing the diffusion parameters.

As noted in the previous figures, the simulated peaks fit quite well the experimental ones, indicating that it was chosen the best fitting parameters, and then it was followed this approach for all calculations. It can also be observed that as it increases the equilibrium constant the peak decreases and is deviating to the right, however increading or reducing the parameters of diffusion it is observed that the diffusion zone (represented in blue) fits poorly, which indicates that it is quite sensitive to variation of these parameters.

It was performed the same type of experiments for methane with the adsorbent in the sodic form, in the following figure is presented, as example, the adjustment of the experimental curves for methane, varying the helium flow at a given temperature. The other adjustments, at the other temperatures are given in Annex.

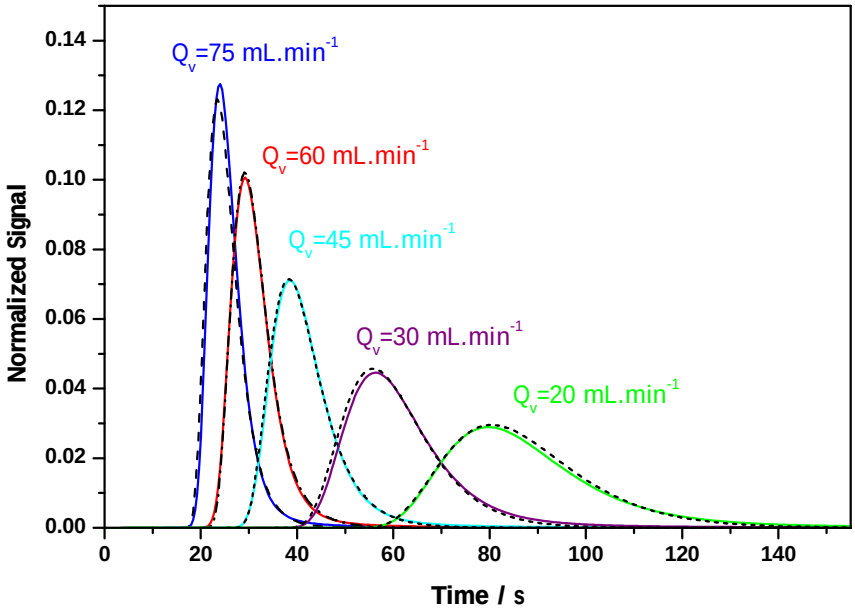

The solid lines correspond to experiments, and the dashed lines are the corresponding simulation

Figure 24: Adjustment of experimental curves of CH_4 in Na-ETS-4 at 25 ° C, varying helium flow.

The following table depicts the values of diffusion parameters for all experiments with methane in Na-ETS-4.

Table 11: Diffusion and adsorption parameters obtained for experiments CH_4 in Na-ETS-4.

T (K)	Q_{He} (mL.min^{-1})	D_c/r_c^2 (s^{-1})	K_H (mol. (Kg.Pa)$^{-1}$)
	77.3	0.038	$1.00.10^{-6}$
	61.2	0.025	$8.00.10^{-7}$
298	46	0.025	$1.00.10^{-6}$
	30.8	0.025	$1.10.10^{-6}$
	20.7	0.018	$9.00.10^{-7}$
	75.6	0.025	$6.00.10^{-7}$
	61.3	0.040	$8.00.10^{-7}$
308	45.7	0.028	$7.00.10^{-7}$
	30.6	0.028	$9.00.10^{-7}$
	21.1	0.023	$9.00.10^{-7}$
	74.7	0.040	$3.00.10^{-7}$
	60	0.040	$4.00.10^{-7}$
323	45.1	∞	$2.00.10^{-7}$
	30.4	∞	$2.00.10^{-7}$
	21.1	∞	$4.00.10^{-7}$

Through the chart above, it is verified that for the temperature of 323 K, it is impossible to measure diffusion, the model fits the experimental peaks for high diffusion rates, hence the meaning of infinity. The equilibrium adsorption constant remains as expected, decreasing when the temperature increases.

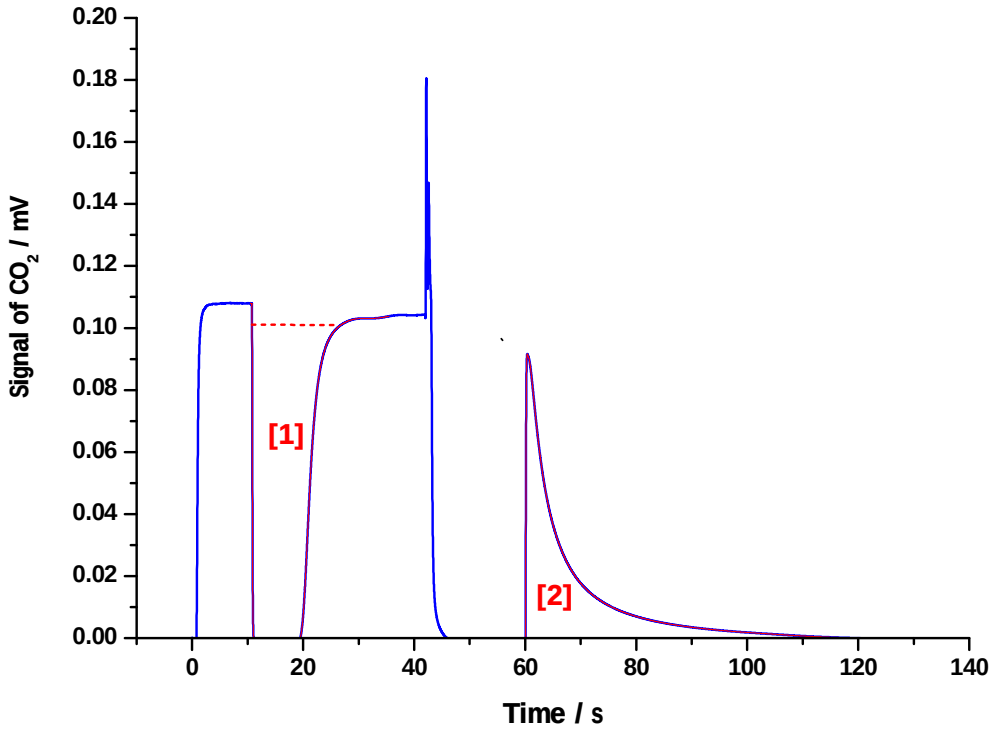

Figure 25: Adsorption experience for CO_2 with Q_{He}= 31.2mL.min-1 in Na-ETS-4.

In this figure the number **1** corresponds to an area that was shown that CO_2 is adsorbed and stay in the solid, break curve, and the number **2** corresponds to desorption curve. It was observed that part of CO_2 has an irreversible adsorption suggesting the presence of very strong adsorption centers. The area in **1** is higher than 2, so it means that part of CO_2, stay in the solid.

In the following figure depicts the adjustment, at a given temperature, for the performed experimental pulses. The remaining adjustments made are present in Annex.

These experiments were carried out after deactivating the irreversible adsorption centers for CO_2 with the experiments commented previously.

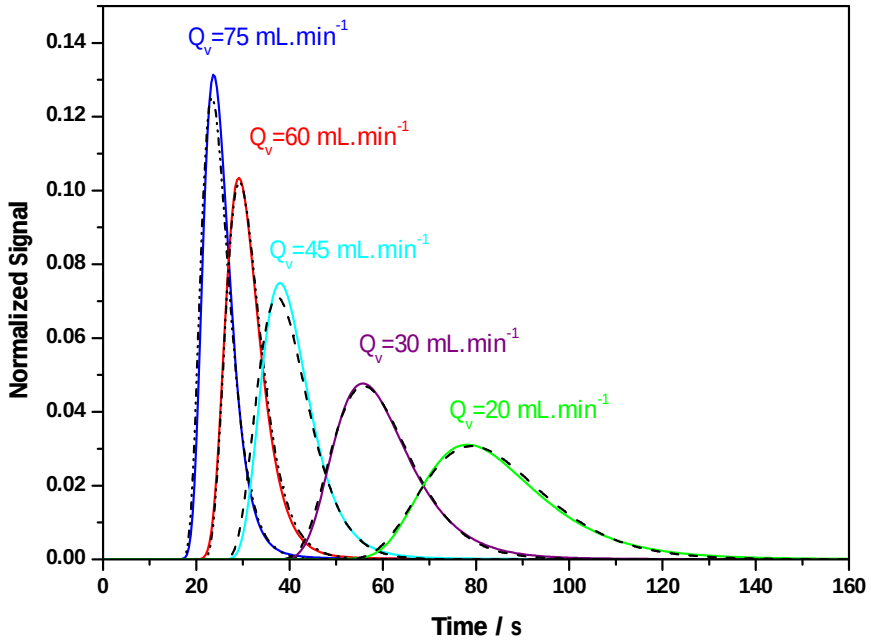

The solid lines correspond to experiments, and the dashed lines are the corresponding simulation

Figure 26: Adjustment of experimental curves of CO_2 in Na-ETS-4 at 25 °C, varying helium flow.

The following table lists the relevant parameters of adsorption and diffusion obtained.

Table 12: Diffusion and adsorption parameters obtained for experiments of CO_2 in Na-ETS-4.

T (K)	Q_{He} (mL.min^{-1})	D_c/r_c^2 (s^{-1})	K_H (mol. (Kg.Pa)$^{-1}$)
298	77.5	0.050	$1.00.10^{-6}$
	61.4	0.035	$8.00.10^{-7}$
	46.7	0.043	$1.20.10^{-6}$
	31.4	0.043	$1.20.10^{-6}$
	21.9	0.043	$1.20.10^{-6}$
308	76.4	0.050	$5.00.10^{-7}$
	61.4	0.050	$7.00.10^{-7}$
	46.4	0.040	$5.00.10^{-7}$
	30.9	0.043	$7.50.10^{-7}$
	21.9	0.048	$1.10.10^{-6}$
323	75.5	0.050	$3.00.10^{-7}$
	60.7	∞	$1.50.10^{-7}$
	46.1	∞	$3.00.10^{-7}$
	30.6	∞	$2.00.10^{-7}$

Such as methane, at 50 ° C it happens the same for CO_2, it is impossible to measure the diffusion because the model presents no variation when exposed to high levels of the diffusion parameters, the equilibrium constant behaves as expected.

4.6.2 Sr-ETS-4

In order to study the parameters of adsorption and diffusion in Sr-ETS-4 for the three gases, it was performed the same type of experiments, using the same methodology as in Na-ETS-4. The following figure presents some adjustments made to a certain temperature for nitrogen, the remaining results are presented in Annex.

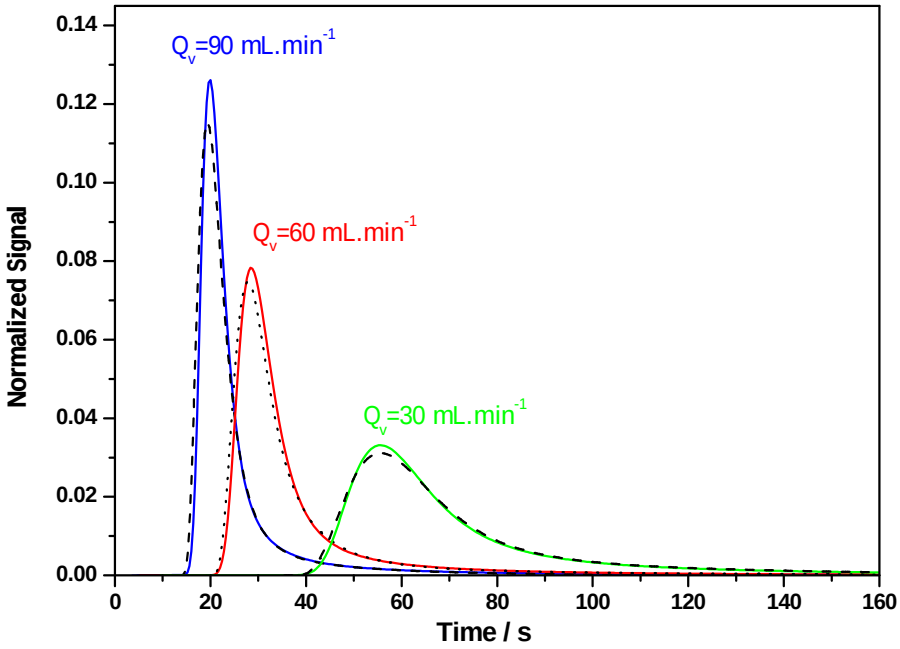

The solid lines correspond to experiments, and the dashed lines are the corresponding simulation

Figure 27: Adjustment of experimental curves of N_2 in Sr-ETS-4 at 25 ° C, varying the helium flow.

The following table shows the parameters obtained adjusting for all the experiments with N_2 at different temperatures.

Table 13: Diffusion and adsorption parameters obtained for experiments N_2 in Sr-ETS-4.

T (K)	Q_{He} (mL.min^{-1})	D_c/r_c^2 (s^{-1})	K_H (mol. (Kg.Pa)$^{-1}$)
298	91.5	0.005	$4.00.10^{-6}$
	61	0.002	$5.50.10^{-6}$
	30.8	0.003	$5.00.10^{-6}$
308	90.8	0.003	$4.20.10^{-6}$
	61.1	0.003	$4.10.10^{-6}$
	30.8	0.003	$4.00.10^{-6}$
323	90.3	0.005	$2.80.10^{-6}$
	60.8	0.005	$2.70.10^{-6}$
	30.5	0.005	$2.60.10^{-6}$

Observing the results shown in Table 13, it is verified that K_H, now in Sr-ETS-4 increased significantly which means that nitrogen adsorbs much more in the solid than in Na-ETS-4, as well as the temperature increases and the constant decreases, as expected. The following figure shows the adjustments of the experiments for methane in Sr-ETS-4.

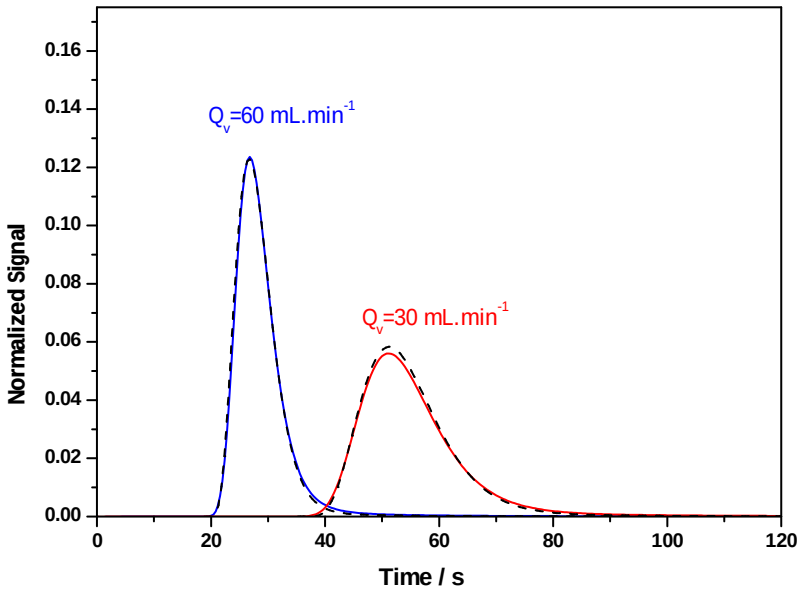

The solid lines correspond to experiments, and the dashed lines are the corresponding simulation

Figure 28: Adjustment of experimental curves of CH_4 in Sr-ETS-4 at 25 °C, varying the helium flow.

Table 14: Diffusion and adsorption parameters obtained for experiments of CH_4 in Sr-ETS-4.

T (K)	Q_{He} (mL.min^{-1})	D_c/r_c^2 (s^{-1})	K_H (mol. (Kg.Pa)$^{-1}$)
298	62.1	0.0010	$5.00.10^{-7}$
	31	0.0010	$5.00.10^{-7}$
308	31.8	0.0010	$5.00.10^{-7}$
	61.8	0.0018	$5.00.10^{-7}$

For the case of methane, it is presented values of K_H, much lower than those presented in the sodic form. This induces that it is adsorbed in lowest quantities. In Sr-ETS-4, it should be noted that in order to have a good separation, these values have a good meaning since nitrogen is adsorbed much more than methane.

There were experiments carried out to 323K but the obtained results were inconclusive.

For carbon dioxide, it was realized the same kind of experiments, having been obtained the adjustments and the parameters of diffusion and adsorption in the following figure and table, respectively.

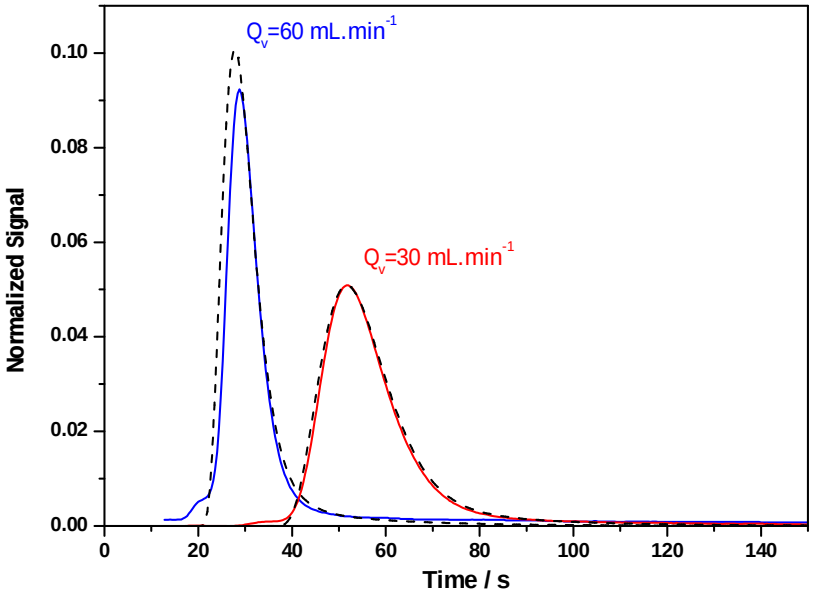

The solid lines correspond to experiments, and the dashed lines are the corresponding simulation

Figure 29: Adjustment of experimental curves of CO_2 in Sr-ETS-4 at 25 °C, varying the Helium flow.

Table 15: Diffusion and adsorption parameters obtained for experiments CO_2 in Sr-ETS-4.

T (K)	Q_{He} (mL.min^{-1})	D_c/r_c^2 (s^{-1})	b (mol. (Kg.Pa)$^{-1}$)
298	63.2	0.0050	1.50E-06
	31.6	0.0050	1.00E-06
308	62.8	0.0055	6.00E-07
	31.5	0.0055	6.00E-07

As provided for carbon dioxide, being a smaller molecule that methane, it is adsorbed also in Sr-4-ETS.

After obtaining the coefficients of transfer of matter (D_c), it was possible to calculate the energy distribution using the following equation:

$$\frac{D_C}{r_c^2} = \frac{D_{C0}}{r_c^2} e^{\left(\frac{-E_{Diff}}{RT}\right)} \quad \textbf{(6)}$$

where Ediff is the energy of diffusion expressed in kJ . mol^{-1}

In the following table are the values of the energies of diffusion to the adsorbent in sodium form (Na-ETS-4) and the adsorbent exchanged with strontium (Sr-ETS-4).

Table 16: Diffusion energy values for both absorbents

Adsorbent	Gases	E_{diff} (kJ.mol^{-1})
Sr-ETS-4	N_2	15.99
	CH_4	24.30
	CO_2	7.27
Na-ETS-4	N_2	13.26
	CH_4	8.16
	CO_2	6.04

Observing the above table can be verified that the diffusion energy is higher in Sr-ETS-4 than in Na-ETS-4. This fact can be explained due to the contraction of the Sr-ETS-4 pores making its diameter smaller, which constitutes a barrier between the molecule to adsorb and the adsorbent, leading to the need of higher diffusion energy to overcome this fact.

Because Methane has a diffusion energy so high in Sr-ETS-4 it is shown that the molecular size (0.38 nm) presents itself as an extra difficulty to the diffusion trough the pores of the adsorbent.

The following table represents a summary of the adsorption parameters obtained and their selectivity for better visualization and comparison of the two adsorbents used.

Table 17: Adsorption parameters and values of selectivity for the 3 gases for both adsorbents.

	NA-ETS-4					Sr-ETS-4				
	N_2	CH_4	CO_2			N_2	CH_4	CO_2		
T	K_H	K_H	K_H	$\alpha_{N2/CH4}$	$\alpha_{CO2/CH4}$	K_H	K_H	K_H	$\alpha_{N2/CH4}$	$\alpha_{CO2/CH4}$
(K)	mol. $(Kg.Pa)^{-1}$					mol. $(Kg.Pa)^{-1}$				
298	$1,20.10^{-6}$	$9,60.10^{-7}$	$1,08.10^{-6}$	1,25	1,13	$4,83.10^{-6}$	$5,00.10^{-7}$	$1,25.10^{-6}$	9,67	2,50
308	$6,43.10^{-7}$	$7,80.10^{-7}$	$7,10.10^{-7}$	0,82	0,91	$4,05.10^{-6}$	$5,00.10^{-7}$	$6,00.10^{-7}$	8,10	1,20
323	$2,17.10^{-7}$	$3,00.10^{-7}$	$2,38.10^{-7}$	0,72	0,79	$2,6.10^{-6}$	-	-	-	-

It was observed in table it was verified that the separation nitrogen / methane, in Sr-ETS-4, is more effective because the selectivity of nitrogen is much better than the methane. As for the separation of carbon dioxide / methane, it was observed the same, the selectivity of CO_2 increases in Sr-ETS-4.

4.7 Analysis of the obtained adsorption and diffusion parameters

Once obtained the adsorption and diffusion parameters of the studied gases in both adsorbents, objective of this work, was done an analysis and comparison between the values determined and those present in literature. For this comparison, in the next table are presented the experimental values for the Na-ETS-4 and the ones found by previous works.

Table 18: Comparison between the values obtained in Na-ETS-4 and the values found in literature, at 298 K.

	This work	**Delgado et al.** [32]	**Marathe et al.** [31]
$K_{H,CH4}$ **(mol.kg^{-1}.Pa^{-1})**	$9.60.10^{-7}$	$3.12 \cdot 10^{-6}$	$4.20 \cdot 10^{-6}$
$K_{H,N2}$ **(mol.kg^{-1}.Pa^{-1})**	$1.20.10^{-6}$	$2.04 \cdot 10^{-6}$	$3.98 \cdot 10^{-6}$
$D_{C,CH4}/r_c^2$ **(s^{-1})**	$2.6.10^{-2}$	$4.0 \cdot 10^{-3}$	$5.0 \cdot 10^{-5}$
$D_{C,N2}/r_c^2$ **(s^{-1})**	$5.3.10^{-2}$	$5.0 \cdot 10^{-2}$	$5.4 \cdot 10^{-5}$
$D_{C,N2}/D_{C,CH4}$	2.04	12.5	1.1

From the table can be realized that the determined values for the Henry constant are higher for nitrogen than for methane, precisely the opposite of the conclusion drawn from the values of other authors. These results suggest that the dehydration temperature of the adsorbent promotes the pore contraction necessary for the application of the adsorbent in the separation of nitrogen/methane.

The obtained values of diffusion coefficient for the nitrogen gas are as the same magnitude of those found by Delgado et al., being much higher than those found by Marathe et al.. This facts is explained because this last author found higher values of diffusion distance in previous works, so for the same value of diffusion a higher value of diffusion constant is found.

For the exchanged adsorbent, Sr-ETS-4, the same analysis was performed, and it's presented in the following table.

Table 19: Comparison between the values obtained in Sr-ETS-4 and the values found in literature, at 298 K.

	This work	**Delgado et al.** [32]	**Marathe et al.** [31]
Temperature (K)	298	298	298
$K_{H,CH4}$ ($mol.kg^{-1}.Pa^{-1}$)	$5.00 \cdot 10^{-7}$	$9.50 \cdot 10^{-7}$	$1.24 \cdot 10^{-6}$
$K_{H,N2}$ ($mol.kg^{-1}.Pa^{-1}$)	$4.83 \cdot 10^{-6}$	$5.32 \cdot 10^{-6}$	$3.43 \cdot 10^{-6}$
$D_{C,CH4}/r_c^2$ (s^{-1})	$1 \cdot 10^{-3}$	$3.2 \cdot 10^{-4}$	$1.08 \cdot 10^{-5}$
$D_{C,N2}/r_c^2$ (s^{-1})	$3 \cdot 10^{-3}$	$7.0 \cdot 10^{-3}$	$3.19 \cdot 10^{-4}$
$D_{C,N2}$ / $D_{C,CH4}$	3.1	21.9	29.5
$(K_{H,N2}/ K_{H,CH4})(D_{C,N2}/D_{C,CH4})^{0.5}$	17.0	26.2	15.0
Excharged Sr (%)	93	93	100
Heating Temperature (ºC)	200	200	310

From the previous table can be observed that the Henry constant values of N_2 are much higher than those obtained for methane, which is in agreement with the values presented in literature. These results show that the heating at 200ºC of the synthesized Sr-ETS-4 by microwaves promotes the pore contraction needed for its application in the nitrogen/methane separation.

The observed differences between the experimental values of this work and the ones found in the literature can be explained by the different adsorbent synthesis methods and to the different chemical composition of the adsorbent.

The diffusion constants are higher for the Na-ETS-4 than for the Sr-ETS-4 adsorbent. These results show the same tendency than those presented in the literature, due to the higher pre-treatment temperature of dehydration used for the Sr-ETS-4 comparatively with the Na-ETS-4, making its pores narrower and leading to a slower diffusion.

5 Conclusions

In this project, the crystals of Na-ETS-4 and Sr-ETS-4 were synthesized by microwaves heating. The DRX analysis for both materials, at different temperatures showed that the two adsorbents lose their structural characteristics at elevated temperatures. However, the adsorbent exchanged with strontium has a higher thermal stability, maintaining a high level of crystallinity up to 200 ºC, while the structure of adsorbent Na-ETS-4 maintains only up to 150 º C.

Adsorption and diffusion parameters for nitrogen, methane and carbon dioxide in Na-ETS-4 and Sr-ETS-4, dehydrated at 150 ºC and 200 ºC, respectively, were estimated by modeling the pulse of each gas that is intended to study, passing a settled helium flow, through a semi-continuous process of fixed bed of crystals of ETS-4.

Analyzing the results, it was observed that Sr-ETS-4, is effective for the separation of N_2/CH_4, since the selectivity of nitrogen is larger than for methane. The differences between the isotherms of CH_4 and N_2 were clear and the obtained values of adsorption capacities for nitrogen are higher than the adsorption capacity for methane.

Such results suggest that the temperature of dehydration used, in both adsorbents, promotes the required contraction of the pore for its application in separating nitrogen/methane. For carbon dioxide, it was estimated the diffusion and adsorption parameters, obtaining consistent values with the literature, despite being sparse. Nevertheless, it was possible to verify that CO_2 adsorbs in greater quantities than methane in Sr-ETS-4 and thus, to conclude that these adsorbents can be useful also for this separation.

The adsorption enthalpy of methane and nitrogen on Na-ET-4 is higher than that obtained for the adsorbent Sr-ETS-4, due the greater repulsion promoted by the contraction of the pores in Sr-ETS-4.

The diffusion constant of nitrogen obtained for the adsorbent Na-ETS-4 were higher than those obtained for the adsorbent Sr-ETS-4. This behavior occurred due the dehydration pre-treatment temperature used for Na-ETS-4 being greater than for adsorbent exchanged with strontium, and consequently, the pores became more contracted and therefore, the diffusion slower.

The two methodologies applied resulted in different adsorption parameters values, but they are of the same order of magnitude and follow the same trend with temperature, with respect to the parameters of adsorption and diffusion on both adsorbents.

6 Evaluation of the work done

6.1 Accomplished objectives

This project had as main objective the calibration and start up of an experimental installation where could be possible:

- Determination of the adsorption isotherms of N_2, CH_4 and CO_2 for the adsorbents Na-ETS-4 and Sr-ETS-4;
- Estimate the diffusion and adsorption parameters of all gases in each adsorbent; this was made using gas pulses, for which was necessary to apply an adequate mathematical model.

After some moths of work, all the objectives proposed were accomplished.

6.2 Limitations and suggestions for future work

The main limitation of this work was that, by the methodology employed, the adsorption and diffusion parameters only have been estimated only for low concentration.

As proposal to future work, the study at higher values of concentration should be done, using larger quantities of adsorbent. The study of EST-4 crystals agglomeration should be done, since in industry is used in this configuration for better separation processes.

6.3 Final appreciation

The fact that this project was done in a foreign country, demanded more initiative and creativity, what was very beneficial as it contributed so much for my autonomy. In these five months, exclusively dedicated to this project, putting all my efforts and dedication in this work, I feel very accomplished with the personal experience gained and with the final results obtained.

References

1 - US-EPA Coalbed Methane Outreach Program. Technical and Economic Assessment of Potencial to Upgrade Gob Gas to Pipeline Quality, Report 430-R-97-012, 1997.

2 - D. M. Ruthven, S. Farooq and K. S. Knaebel, *Pressure Swing Adsorptio*n; VCH, New York, 1994.

3 - D. W. Breck, *Zeolite Molecular Sie es: Structure, Chemistry and Us*e, John Wiley, New York, 1974.

4 - S. M. Kuznicki, US Patent 4,938,939, 1990.

5 - S. M. Kuznicki, V. A. Bell, S. Nair, H. W. Hillhouse, R. M. Jacubinas, C. M. Braunbarth, B. H. Toby and M. Tsapatsis, *Nature*, *41*2 (6848), 720-724 (2001).

6 - Gás Natural, http://www.gasnatural.com, Access in June 2010.

7 - British Petroleum (BP). Revisão Estatística de Energia Mundial – June 2010

8 - Deutsche BP, http://www.deutsch.de/liveassets, Access in June 2010

9 - Engelhard Corporation, Adsorption Processes for Natural Gas Treatment, A Technology Update, www.engelhard.com, 2005.

10 - Lozano-Castello, D.; Cazorla-Amoros, D.; Linares-Solano, A.; Quinn, D. F.Micropore Size Distributions of Activated Carbons and Carbon Molecular Sieves Assessed by High-Pressure Methane and Carbon Dioxide Adsorption Isotherms. *J.Phys. Chem. B*, 2002, 106, 9372-9379.

11 - http://www.biodieselbr.com/energia/biogas/biogas.htm access in June 2010.

12 - Persson M. "Biogas – a renewable fuel for the transport sector for the present and the future" SGC, www.sgc.se, access March de 2010.

13 - http://www.bbc.co.uk/portuguese/especial/1931_energia/index.shtml access in June 2010.

14 - http://tv1.rtp.pt/noticias/?article=89563&visual=3&layout=10, access in June 2010.

15 - Engelhard Corporation. Purification Technologies Brochure, 2003.

16 - Arruebo, M.; Coronas, J.; Menéndez, M.; Santamaria, J.Separation of hydrocarbons from natural gas using silicalite membranes. *Sep. Pur. Tech.*, 2001, 25,275-286.

17 - EDP, http://www.edp.pt/EDPI/Internet/PT/Group/AboutEDP /BusinessEnvironment/ GasinIberia /GasPT.htm, access in June 2010.

18 - Portugal em grande, http://www.portugalemgrande.com/?q=node/4207, Access in June 2010

19 - Engelhard Corporation, Adsorption Processes for Natural Gas Treatment, A Technology Update, www.engelhard.com, 2005.

20 - Da Silva, F.A.Cyclic Adsorption Processes: Application to Propane/Propylene Separation. Ph.D. Dissertation, University of Porto, Portugal, 1999.

21 - Ruthven, D.M.Principles of adsorption and adsorption processes.Wiley, NewYork, 1984.

22 - Tondeur, D.; Wankat, P. C. Gas Purification by PSA. *Sep. & Pur. Meth.*, 1985, 14, 157-212.

23 - Yang, R. T. Gas Separation by Adsorption Processes. Butterworths, Boston, 1987.

24 - Suzuki, M. Adsorption Engineering; Chemical Engineering Monographs Elsevier

Tokyo, 1990.

25 - Nataraj, S.; Wankat, P. C. Multicomponent Pressure Swing Adsorption. In Recent Advances in Adsorption and Ion Exchange. AIChE, New York, 1982, 78, 29-38

26 - Cen, P. L.; Yang, R. T. Separation of a five-component gas mixture by Pressure Swing Adsorption. *Sep. Sci. Tech.*, Nov-Dec 1985, 20, 725-747.

27 - R. T. Yang, *Adsorbents: Fundamentals and Application*s; John Wiley, NewJersey, 2003.

28 - S. M. Kuznicki, US Patent 4,938,939, 1990.

29 - S. M. Kuznicki, V. A. Bell, I. Petrovic and B. T. Desai, US Patent 6,068,682, 2000.

30 - Jayaraman, A.J. Hernández-Maldonado, R. T. Yang,D. Chinn, C.L. Munson and D. H. Mohr, *Chem. Eng. Sci.*, *5*9, 2407-2417 (2004).

31 - R. P. Marathe, S. Farooq and M. P. Srinivasan, *Langmuir*, *2*1 (10), 4532-4546 (2005).

32 - J. A. Delgado, M. A. Uguina, V. I. Agueda and A. G. Sanz, Langmuir, 24, 6107-6115 (2008).

33 - J.A. Delgado, M. A. Uguina, J.L. Sotelo, B. Ruiz and J.M. Gómez, *Adsorption*, *12*, 5-18 (2006).

34 - F. da Silva and A. E. Rodrigues, *AIChE Journal*, *47*, 341-357 (2001).

35 - N.K. Madsen and R.F. Sincovec, *ACM Transactions on Mathematical Software*, 5 (3), 326-351 (1976).

36 - J. A. Delgado, T. A. Nijhuis, F. Kapteijn and J. A. Moulijn, *Chem. Eng.Sci.*, *5*7, 1835-1847 (2002).

37 - D. Coutinho, J. A. Losilla and K.J. Balkus, Jr. *Microporous and Mesoporous Materials.*, *9*0, 229-236 (2006).

38- Cavenati et al., *Microporous and Mesoporous Materials*, Adsoption of small molecules on alkali-earth modified titanosilicates, 121(1-3) 114-120 (2009)

Annex

Annex A: Calibration

A.1: N_2

Table A.1.1: Experimental data for the calibration pulses of nitrogen.

Q_{helio} (mL.min^{-1})	Volume (mL)	Area (mV·s)	n_{CH4} (moles)	Q.Area (mV·s·mL.min^{-1})
30	0.05	$8.9 \cdot 10^{4}$	$9.57 \cdot 10^{-7}$	$2.78 \cdot 10^{6}$
	0.1	$1.8 \cdot 10^{5}$	$1.91 \cdot 10^{-6}$	$5.46 \cdot 10^{6}$
	0.25	$3.4 \cdot 10^{5}$	$3.83 \cdot 10^{-6}$	$1.05 \cdot 10^{7}$
	0.5	$1.7 \cdot 10^{6}$	$1.91 \cdot 10^{-5}$	$5.45 \cdot 10^{7}$
60	0.05	$4.5 \cdot 10^{4}$	$9.57 \cdot 10^{-7}$	$2.76 \cdot 10^{6}$
	0.1	$8.7 \cdot 10^{4}$	$1.91 \cdot 10^{-6}$	$5.39 \cdot 10^{6}$
	0.25	$1.7 \cdot 10^{5}$	$3.83 \cdot 10^{-6}$	$1.08 \cdot 10^{7}$
	0.5	$8.7 \cdot 10^{5}$	$1.91 \cdot 10^{-5}$	$5.39 \cdot 10^{7}$
90	0.05	$2.9 \cdot 10^{4}$	$9.57 \cdot 10^{-7}$	$2.73 \cdot 10^{6}$
	0.1	$5.8 \cdot 10^{4}$	$1.91 \cdot 10^{-6}$	$5.41 \cdot 10^{6}$
	0.25	$1.2 \cdot 10^{5}$	$3.83 \cdot 10^{-6}$	$1.11 \cdot 10^{7}$
	0.5	$5.8 \cdot 10^{5}$	$1.91 \cdot 10^{-5}$	$5.40 \cdot 10^{7}$

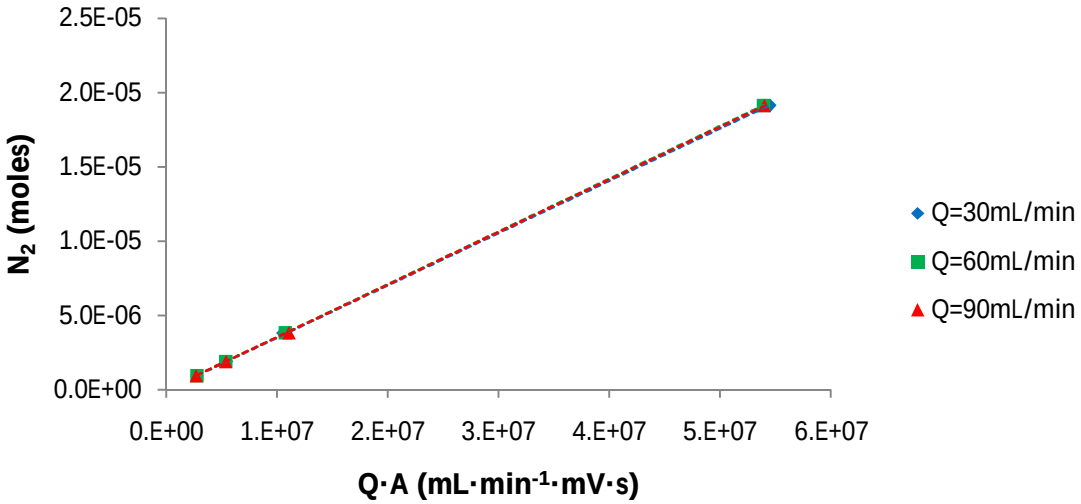

Figure A.1.1: Calibration curve for pulse of N_2, varying the helium flow.

A.2: CH_4

Table A.1.2: Experimental data for the calibration pulses of methane.

Q_{helio} (mL.min^{-1})	Volume (mL)	Area (mV·s)	n_{N2} (moles)	Q.Area (mV·s·mL.min^{-1})
30	0.05	$8.6 \cdot 10^{4}$	$9.57 \cdot 10^{-7}$	$2.70 \cdot 10^{6}$
	0.1	$1.7 \cdot 10^{5}$	$1.91 \cdot 10^{-6}$	$5.43 \cdot 10^{6}$
	0.25	$3.4 \cdot 10^{5}$	$3.83 \cdot 10^{-6}$	$1.05 \cdot 10^{7}$
	0.5	$1.7 \cdot 10^{6}$	$1.91 \cdot 10^{-5}$	$5.25 \cdot 10^{7}$
60	0.05	$4.4 \cdot 10^{4}$	$9.57 \cdot 10^{-7}$	$2.72 \cdot 10^{6}$
	0.1	$8.7 \cdot 10^{4}$	$1.91 \cdot 10^{-6}$	$5.38 \cdot 10^{6}$
	0.25	$1.7 \cdot 10^{5}$	$3.83 \cdot 10^{-6}$	$1.06 \cdot 10^{7}$
	0.5	$8.6 \cdot 10^{5}$	$1.91 \cdot 10^{-5}$	$5.32 \cdot 10^{7}$
90	0.05	$2.9 \cdot 10^{4}$	$9.57 \cdot 10^{-7}$	$2.72 \cdot 10^{6}$
	0.1	$5.7 \cdot 10^{4}$	$1.91 \cdot 10^{-6}$	$5.32 \cdot 10^{6}$
	0.25	$1.1 \cdot 10^{5}$	$3.83 \cdot 10^{-6}$	$1.06 \cdot 10^{7}$
	0.5	$5.7 \cdot 10^{5}$	$1.91 \cdot 10^{-5}$	$5.30 \cdot 10^{7}$

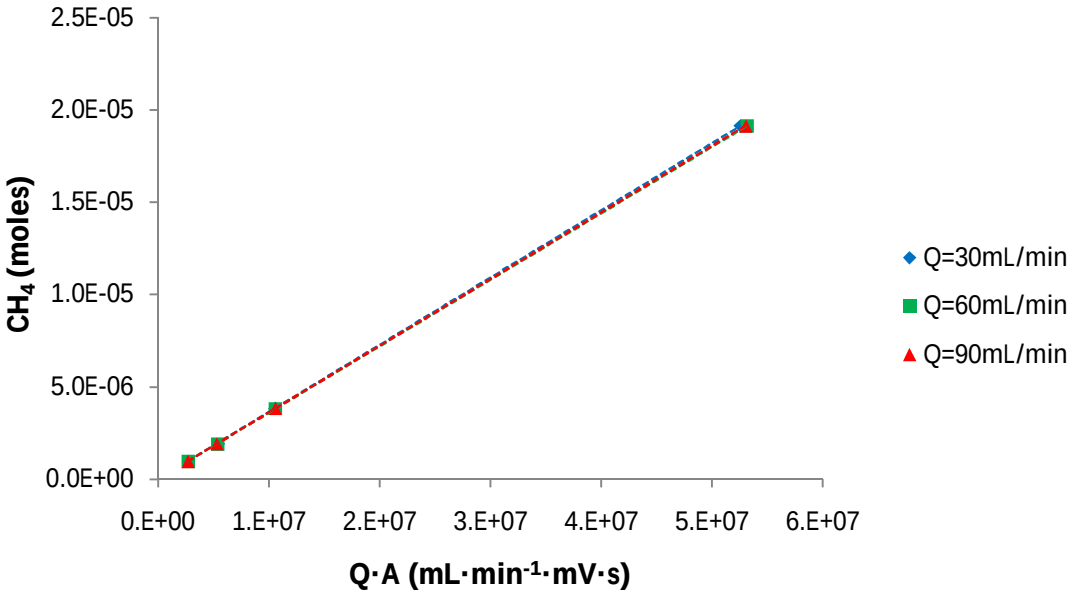

Figure A.1.2 : Calibration curve for pulse of CH_4, varying the helium flow.

A.3: CO_2

Table A.1.3: Experimental data for the calibration pulses of carbon dioxide.

Q_{helio} (mL.min^{-1})	Volume (mL)	Area (mV·s)	n_{N2} (moles)	Q.Area (mV·s·mL.min^{-1})
30	0.05	$4.3 \cdot 10^{4}$	$9.41 \cdot 10^{-7}$	$2.40 \cdot 10^{6}$
	0.1	$8.4 \cdot 10^{4}$	$1.88 \cdot 10^{-6}$	$4.81 \cdot 10^{6}$
	0.25	$1.8 \cdot 10^{5}$	$3.76 \cdot 10^{-6}$	$9.57 \cdot 10^{6}$
	0.5	$7.7 \cdot 10^{5}$	$1.88 \cdot 10^{-5}$	$4.58 \cdot 10^{7}$
60	0.05	$4.0 \cdot 10^{4}$	$9.41 \cdot 10^{-7}$	$2.46 \cdot 10^{6}$
	0.1	$8.0 \cdot 10^{4}$	$1.88 \cdot 10^{-6}$	$4.92 \cdot 10^{6}$
	0.25	$1.6 \cdot 10^{5}$	$3.76 \cdot 10^{-6}$	$9.96 \cdot 10^{6}$
	0.5	$7.7 \cdot 10^{5}$	$1.88 \cdot 10^{-5}$	$4.76 \cdot 10^{7}$
90	0.05	$3.9 \cdot 10^{4}$	$9.41 \cdot 10^{-7}$	$2.36 \cdot 10^{6}$
	0.1	$7.9 \cdot 10^{4}$	$1.88 \cdot 10^{-6}$	$4.76 \cdot 10^{6}$
	0.25	$1.5 \cdot 10^{5}$	$3.76 \cdot 10^{-6}$	$9.35 \cdot 10^{6}$
	0.5	$7.6 \cdot 10^{5}$	$1.88 \cdot 10^{-5}$	$4.61 \cdot 10^{7}$

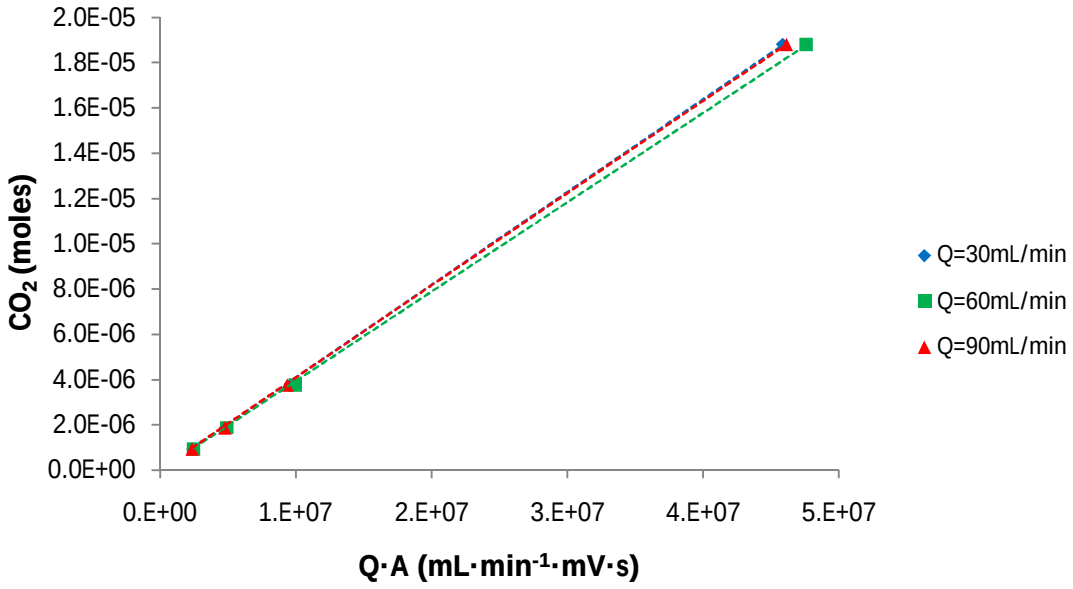

Figure A.1.3: Calibration curve for pulse of CO_2, varying the helium flow.

Annex B: Dead Volume

B.1: He

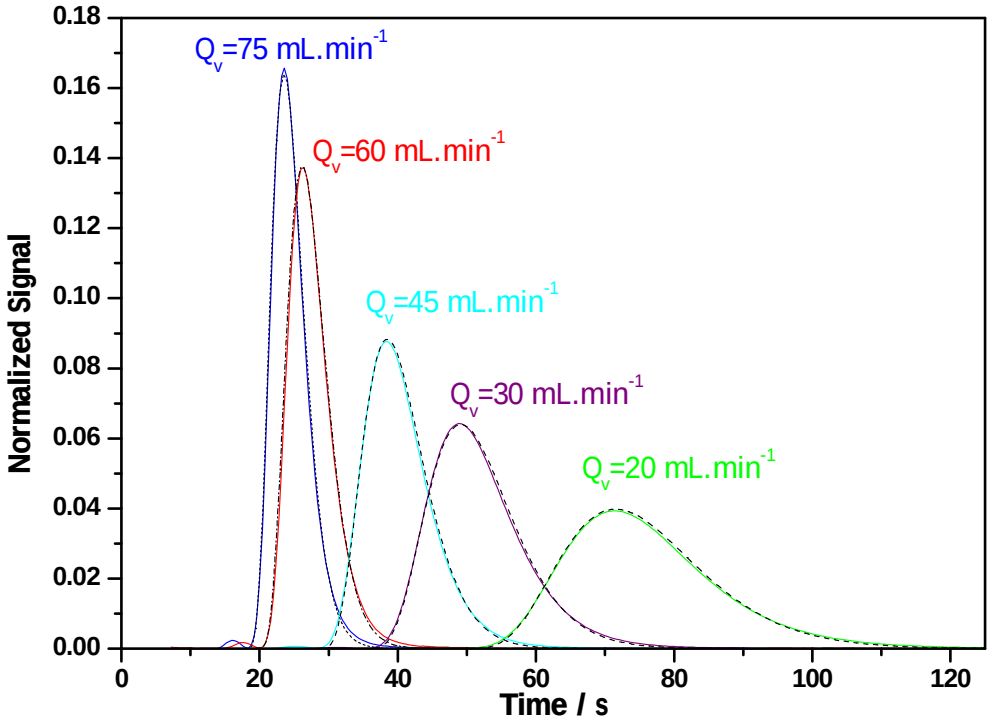

The solid lines correspond to experiments, and the dashed lines are the corresponding simulation

Figure B.1.1: Adjustment of the helium peaks with QN_2=2.23mL.min^{-1} at 308 K.

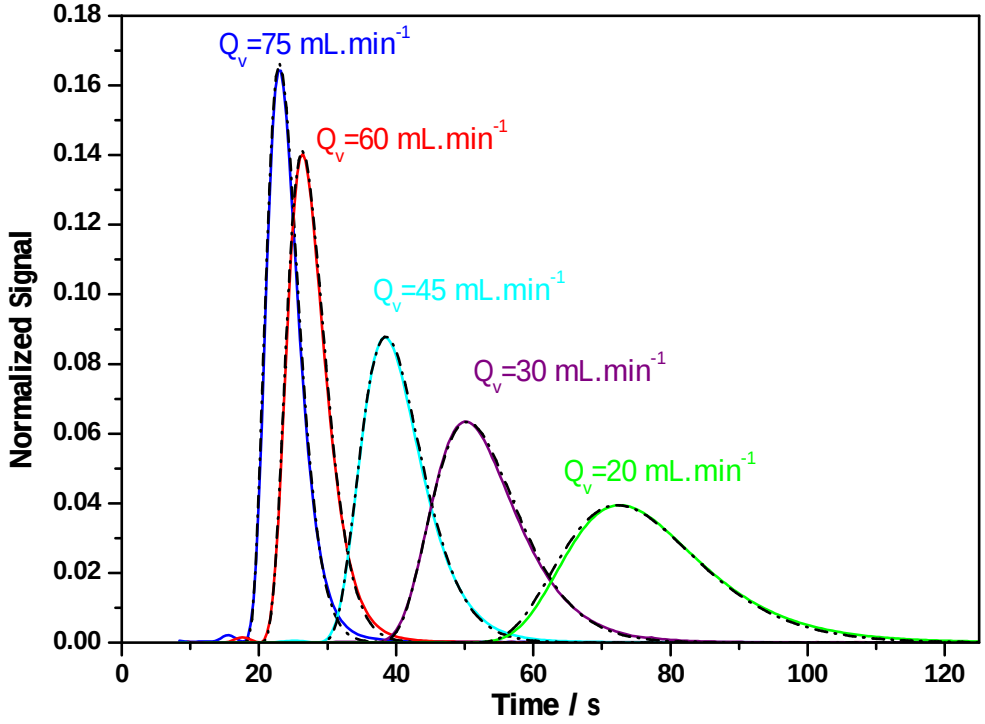

The solid lines correspond to experiments, and the dashed lines are the corresponding simulation

Figure B.1.2: Adjustment of the helium peaks with QN_2=2.23mL.min^{-1} at 323 K.

Annex C: Na-ETS-4

C.1: N_2

Table C.1.1: Experimental values for the nitrogen isotherms in Na-ETS-4.

T_i (K)	Q_{He} ($mL.min^{-1}$)	Q_{N2} ($mL.min^{-1}$)	x_i	P_i (Pa)	N_{ads} (moles)
	22.07	2.23	0.092	8590.57	0.0328
	31.19	2.23	0.067	6240.18	0.0242
	47.42	2.23	0.045	4204.41	0.0161
298	62.17	2.23	0.035	3241.55	0.0121
	77.71	2.23	0.028	2611.15	0.0102
	89.12	2.23	0.024	2299.04	0.0074
	108.09	2.23	0.020	1903.77	0.0074
	22.58	2.23	0.090	8394.30	0.0231
	31.89	2.23	0.065	6104.99	0.0153
	47.31	2.23	0.045	4210.33	0.0102
308	63.06	2.23	0.034	3194.48	0.0069
	76.76	2.23	0.028	2640.39	0.0066
	94.90	2.23	0.023	2147.16	0.0066
	111.27	2.23	0.020	1837.52	0.0064
	22.51	2.23	0.090	8445.88	0.0094
	31.39	2.23	0.066	6216.71	0.0052
	46.46	2.23	0.046	4291.73	0.0034
323	62.66	2.23	0.034	3220.35	0.0029
	76.91	2.23	0.028	2640.72	0.0022
	91.41	2.23	0.024	2242.93	0.0020
	106.13	2.23	0.021	1938.10	0.0025

C.2: CH_4

Table C.2.1: Experimental values for the methane isotherms in Na-ETS-4.

Ti (K)	Q_{He} ($mL.min^{-1}$)	Q_{CH4} ($mL.min^{-1}$)	x_i	P_i (Pa)	N_{ads} (moles)
298	21.45	1.42	0.044	4207.42	0.0154
	45.63	1.42	0.030	2863.12	0.0109
	60.34	1.42	0.023	2181.28	0.0097
	74.47	1.42	0.019	1774.91	0.0073
	91.30	1.42	0.015	1452.78	0.0067
	104.35	1.42	0.013	1273.58	0.0060
308	21.98	1.42	0.061	5761.44	0.0154
	31.33	1.42	0.043	4116.15	0.0120
	46.86	1.42	0.029	2768.21	0.0083
	62.45	1.42	0.022	2092.80	0.0066
	75.98	1.42	0.018	1726.83	0.0051
	93.85	1.42	0.015	1403.00	0.0050
	107.40	1.42	0.013	1238.92	0.0070
323	21.98	1.42	0.061	5688.91	0.0121
	31.01	1.42	0.044	4104.12	0.0091
	48.22	1.42	0.029	2681.57	0.0071
	62.01	1.42	0.022	2098.46	0.0054
	77.25	1.42	0.018	1691.93	0.0043
	93.77	1.42	0.015	1398.29	0.0040
	107.40	1.42	0.013	1223.22	0.0033

Annex D: Sr-ETS-4

D.1: N_2

Table D.1.1: Experimental values for the nitrogen isotherms in Sr-ETS-4.

Ti (K)	Q_{He} (mL.min^{-1})	Q_{N2} (mL.min^{-1})	x_i	P_i (Pa)	N_{ads} (moles)
298	21.24	2.23	0.095	8898.15	0.0513
	30.56	2.23	0.068	6368.38	0.0374
	46.11	2.23	0.046	4319.75	0.0260
	61.78	2.23	0.035	3262.11	0.0214
	76.47	2.23	0.028	2653.26	0.0178
	91.28	2.23	0.024	2232.96	0.0155
308	21.61	2.23	0.093	8771.67	0.0417
	30.49	2.23	0.068	6390.05	0.0300
	46.01	2.23	0.046	4334.88	0.0217
	61.48	2.23	0.035	3281.90	0.0171
	76.76	2.23	0.028	2659.03	0.0143
	91.15	2.23	0.024	2242.36	0.0129
323	21.43	2.23	0.094	8850.04	0.0332
	30.50	2.23	0.068	6398.63	0.0223
	45.55	2.23	0.047	4361.05	0.0164
	61.32	2.23	0.035	3278.50	0.0136
	76.33	2.23	0.024	2652.33	0.0113
	91.25	2.23	0.094	2228.92	0.0097

Annex E: Estimation of adsorption and diffusion parameters

E.1:Na-ETS-4

E.1.1:N_2

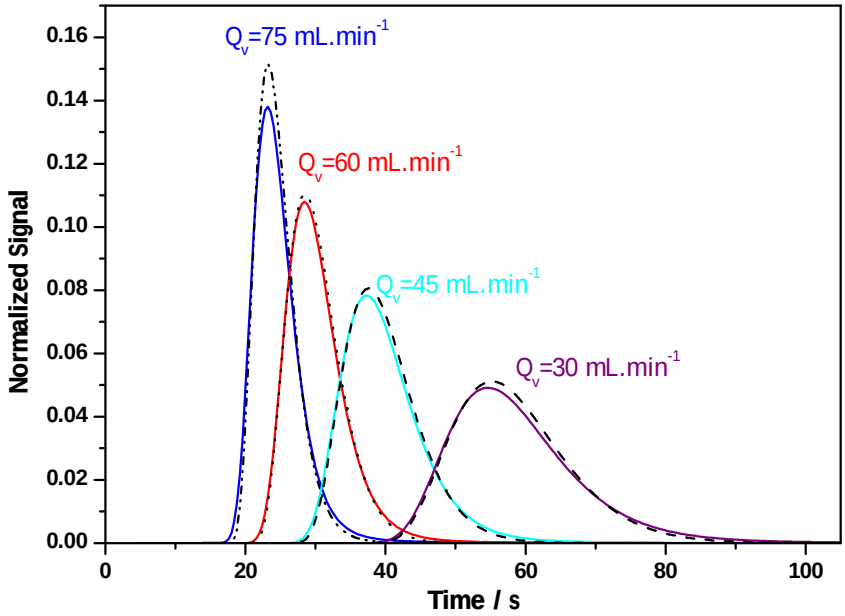

The solid lines correspond to experiments, and the dashed lines are the corresponding simulation

Figure E.1.1. 1: Adjustment of experimental curves of N_2 Na-ETS-4 at 35 ºC, varying helium flow.

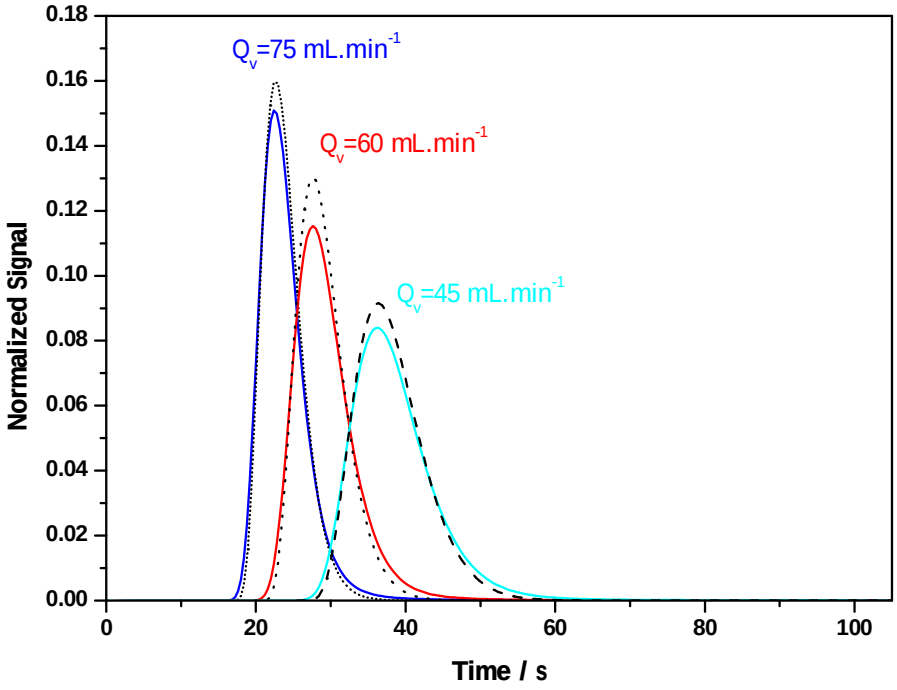

The solid lines correspond to experiments, and the dot lines are the corresponding simulation

Figure E.1.1. 2: Adjustment of experimental curves of N_2 Na-ETS-4 at 50 ºC, varying helium flow.

E.1.2:CH_4

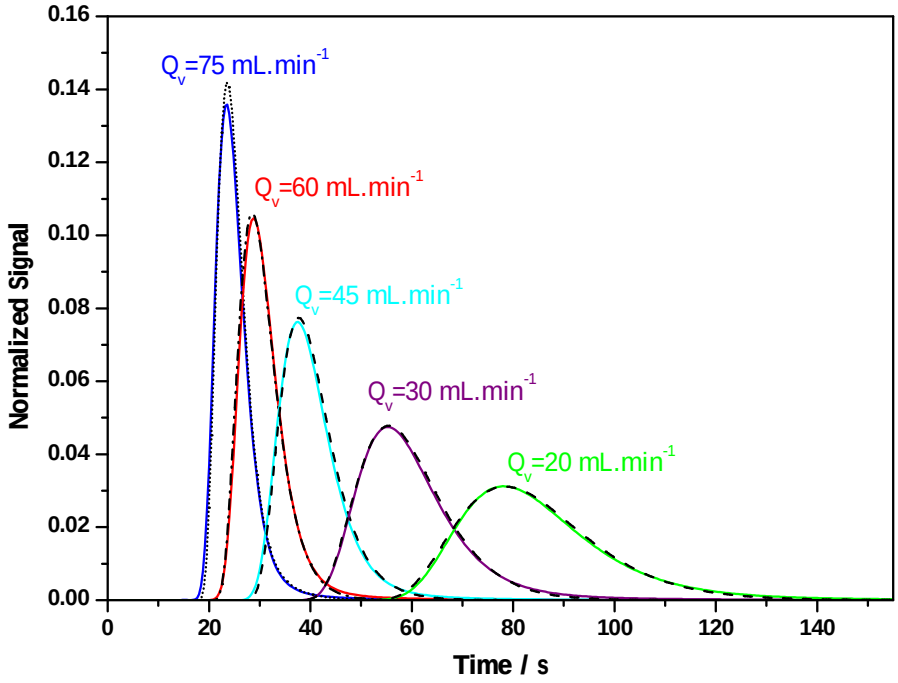

The solid lines correspond to experiments, and the dashed lines are the corresponding simulation

Figure E.1.2. 1: Adjustment of experimental curves of CH_4 Na-ETS-4 at 35 ºC, varying helium flow.

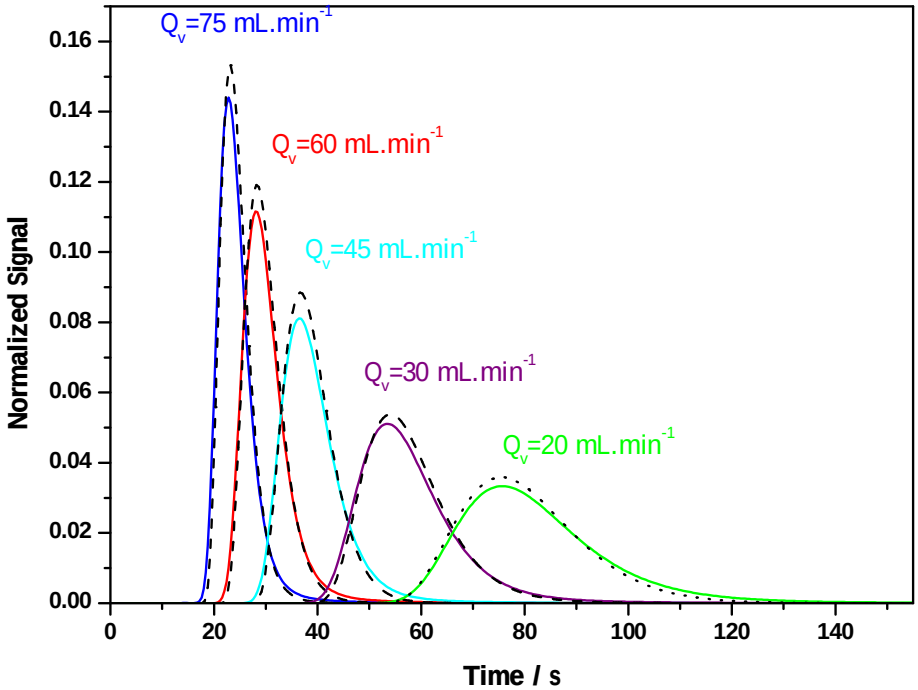

The solid lines correspond to experiments, and the dot lines are the corresponding simulation

Figure E.1.2. 2: Adjustment of experimental curves of CH_4 Na-ETS-4 at 50 ºC, varying helium flow.

E.1.3:CO_2

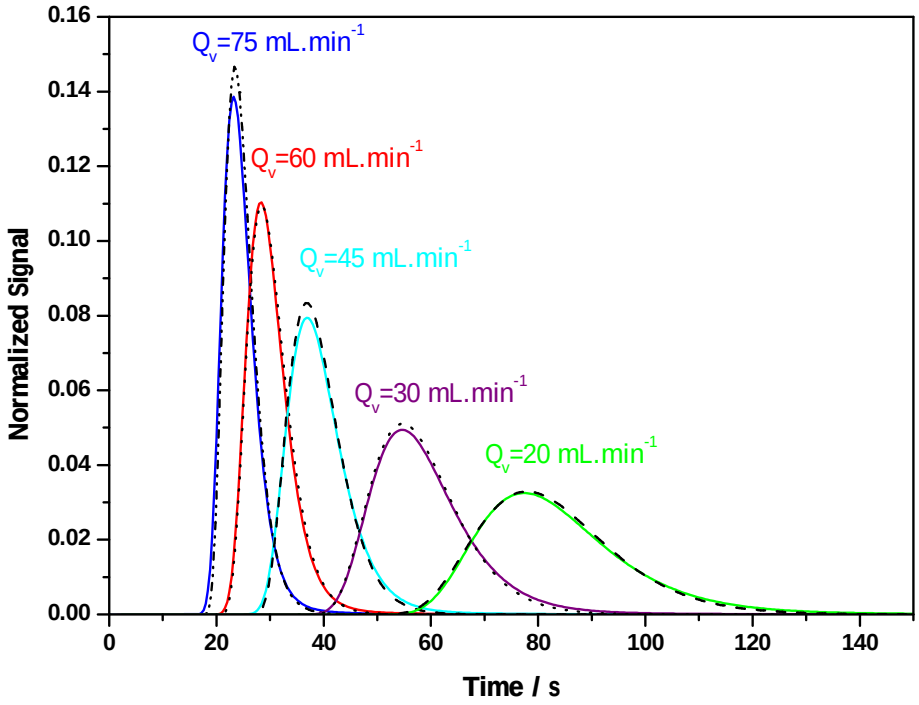

The solid lines correspond to experiments, and the dashed lines are the corresponding simulation

Figure E.1.3. 1: Adjustment of experimental curves of CO_2 Na-ETS-4 at 25 ºC, varying helium flow.

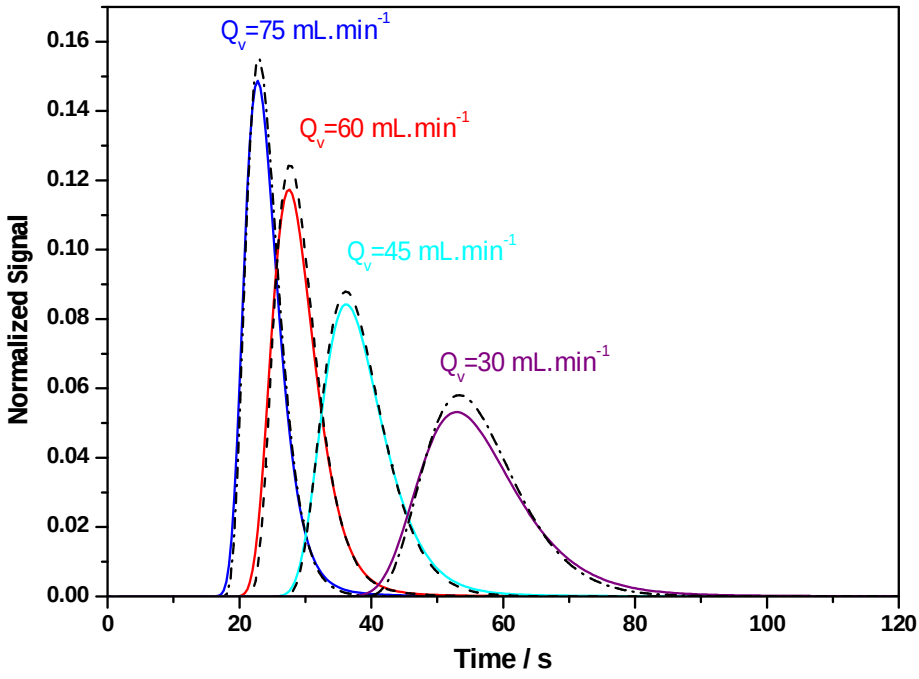

The solid lines correspond to experiments, and the dashed lines are the corresponding simulation

Figure E.1.3. 2: Adjustment of experimental curves of CO_2 Na-ETS-4 at 50 ºC, varying helium flow.

E.2:Sr-ETS-4

E.2.1:N_2

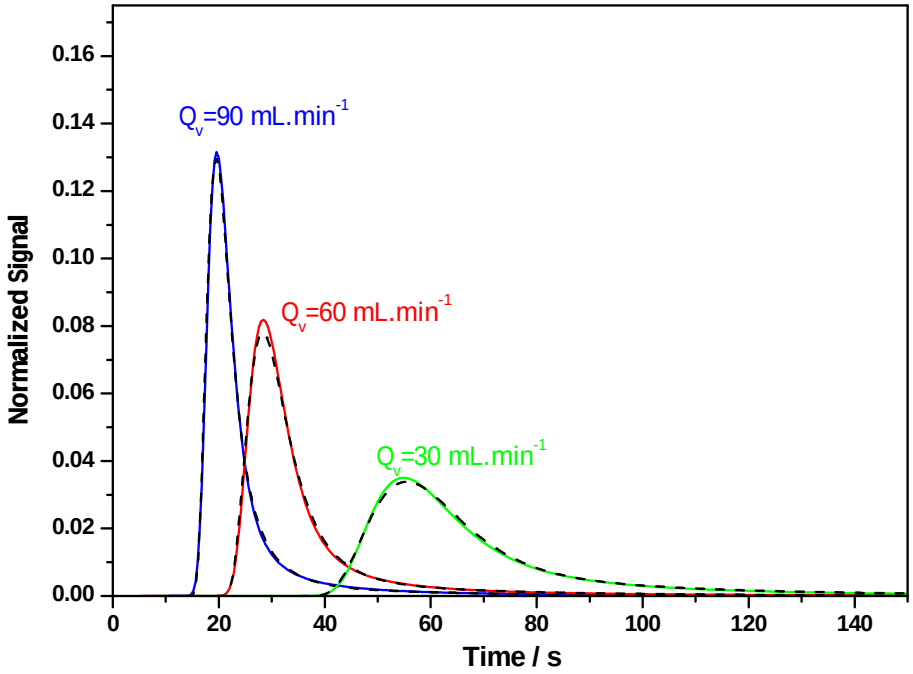

The solid lines correspond to experiments, and the dashed lines are the corresponding simulation

Figure E.2.1. 1: Adjustment of experimental curves of N_2 Sr-ETS-4 at 35 ºC, varying helium flow.

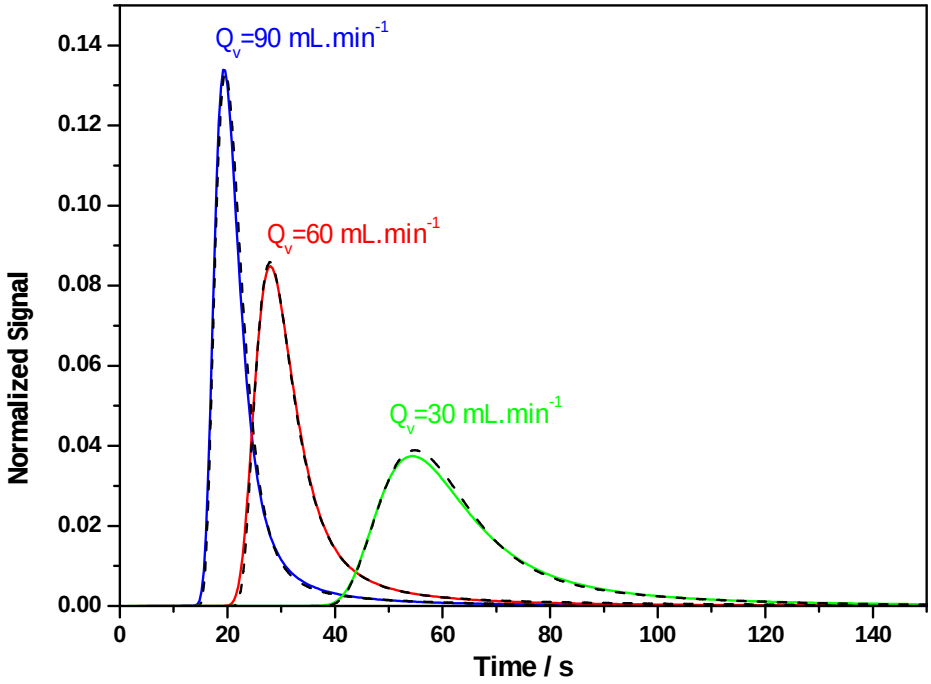

The solid lines correspond to experiments, and the dashed lines are the corresponding simulation

Figure E.2.1. 2: Adjustment of experimental curves of N_2 Sr-ETS-4 at 50 ºC, varying helium flow.

E.2.2:CH_4

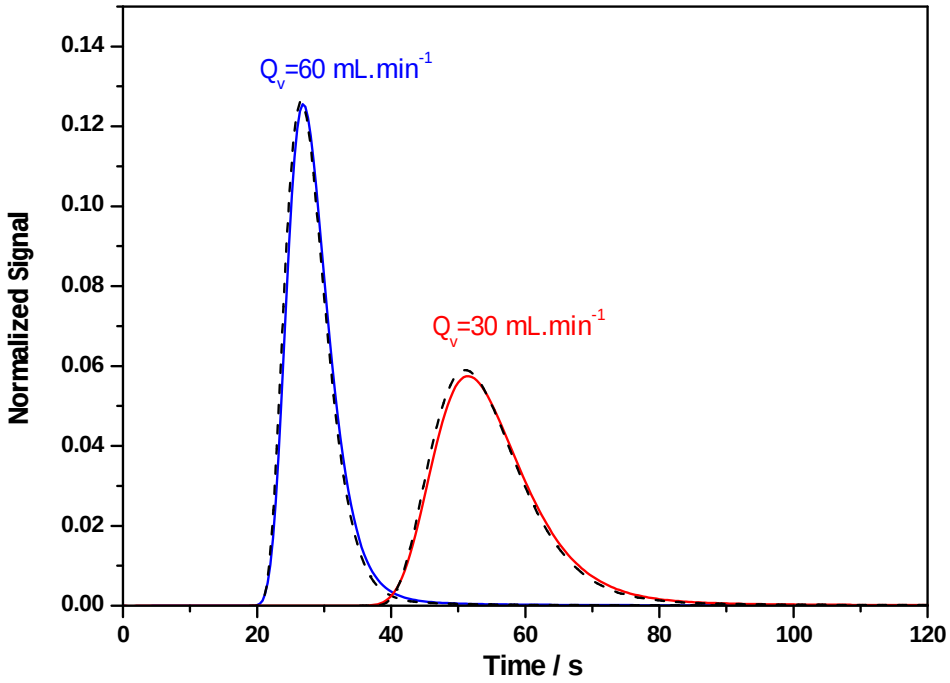

The solid lines correspond to experiments, and the dashed lines are the corresponding simulation

Figure E.2.2. 1 : Adjustment of experimental curves of CH_4 Sr-ETS-4 at 35 ºC, varying helium flow.

E.2.3:CO_2

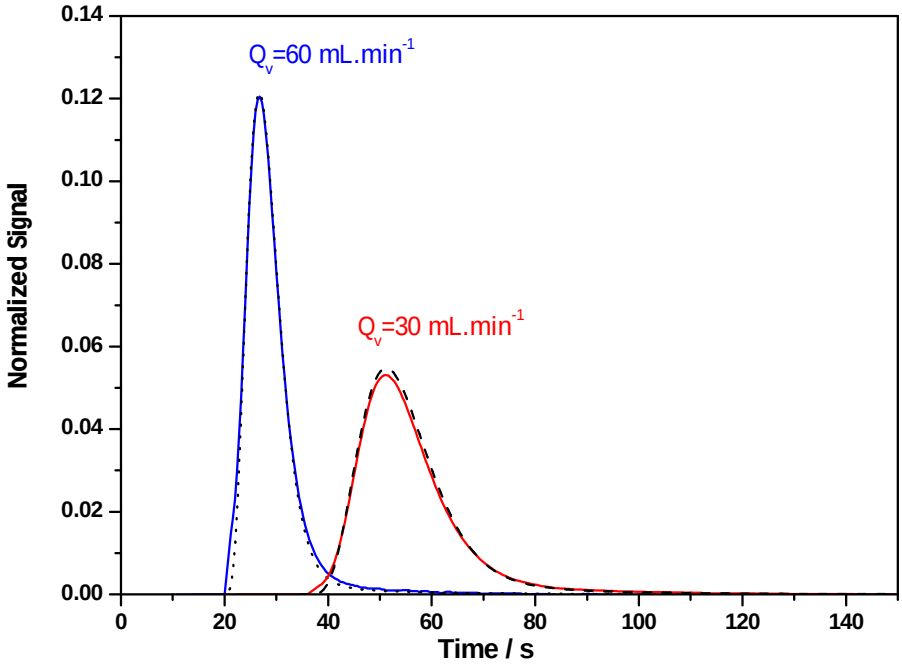

The solid lines correspond to experiments, and the dashed lines are the corresponding simulation

Figure E.2.3. 1: Adjustment of experimental curves of CO_2 Sr-ETS-4 at 35 ºC, varying helium flow.